

國立交通大學

生物科技系所

碩士論文

奈米線場效電晶體生物感測器於腸病毒 71 型
之高靈敏度、無標記且即時檢測

Poly Silicon Nanowire Field Effect Transistor
for High Sensitivity, Label-Free and Rapid Detection of Enterovirus 71

研究生：賴音汝

指導教授：楊裕雄 教授

中華民國九十八年七月

奈米線場效電晶體生物感測器於腸病毒 71 型
之高靈敏度、無標記且即時檢測
Poly Silicon Nanowire Field Effect Transistor
for High Sensitivity, Label-Free and Rapid Detection of Enterovirus 71

研究生：賴音汝

Student：Yin-Ju Lai

指導教授：楊裕雄

Advisor：Yuh-Shyong Yang



Submitted to Department of Biological Science and Technology
College of Biological Science and Technology
National Chiao Tung University
in partial fulfillment of the Requirements
for the Degree of
Master
in

Biological Science and Technology

July 2009

Hsinchu, Taiwan, Republic of China

中華民國九十八年七月

奈米線場效電晶體生物感測器於腸病毒 71 型
之高靈敏度、無標記且即時檢測

學生：賴音汝

指導教授：楊裕雄 教授

國立交通大學生物科技學系(研究所)碩士班

摘 要

對世界各地的幼童而言腸病毒七十一型 (Enterovirus 71, EV71) 是一種重要的致病原且比其他非小兒麻痺腸病毒 (non-polio enterovirus) 具有高致病率及致死率，其感染屬於神經性症狀，且平均會在三天內惡化。傳統的臨床確認檢驗方式需要先病毒培養再進行病毒分離 (virus isolation) 和藉由反轉錄聚合酶鏈式反應 (RT-PCR)，這些過程耗時、昂貴且無法達到立即診斷 EV71。在文獻中，多晶矽奈米線場效電晶體 (polysilicon nanowire field-effect transistor, poly SiNW-FET) 可被製成且具有高靈敏度、無標誌且立即偵測腸病毒七十一型的置能轉換器 (transducer)。對特定 EV71 的 DNA 序列有專一性的單股 DNA 序列先被固定

在多晶矽奈米線場效電晶體表面，用來偵測 EV71 的多晶矽奈米線場效電晶體具有高靈敏度，且能對 EV71 產生反應，並且在有無交互作用的離子分子下仍是穩定的，最低可偵測到 aM (attomolar, aM, 10^{-18} M) 範圍。此結果表示多晶矽奈米線場線電晶體具有靈敏、無標誌且可立即偵測的淺能，此特性可發展成生物感測系統用來偵測 EV71 的感染，以便早期發現早期治療，

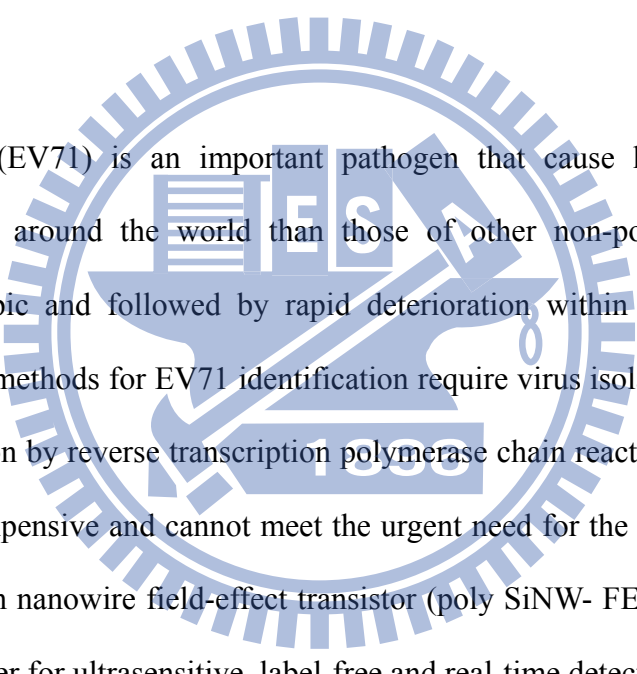
Poly Silicon Nanowire Field Effect Transistor for High Sensitivity, Label-Free and Rapid Detection of Enterovirus 71

Student: Yin-Ju Lai

Advisor: Dr. Yuh-Shyong Yang

Department of Biological Science and Technology
National Chiao Tung University

ABSTRACT



Enterovirus 71 (EV71) is an important pathogen that cause higher morbidity and mortality in children around the world than those of other non-polio enteroviruses. Its infection is neurotropic and followed by rapid deterioration within average 3 days. The conventional clinical methods for EV71 identification require virus isolation from cell culture and DNA amplification by reverse transcription polymerase chain reactions (RT-PCR), which is time-consuming, expensive and cannot meet the urgent need for the diagnosis of EV71. In this report, polysilicon nanowire field-effect transistor (poly SiNW- FET) was fabricated and function as a transducer for ultrasensitive, label-free and real-time detection of EV71. Specific single-strand DNA sequences that the unique DNA sequence of EV71 were first immobilized on poly SiNW-FET. The fabricated poly SiNW-FET based EV71 biosensor exhibit a high sensitive and specific in respond to EV71. The functionalized poly SiNW-FET was stable in the presence of non-interacting ion molecules and was able to detect EV71 RNA at the aM range. The results of this study suggest that the poly SiNW-FET has a potential to be useful developed to a real-time, sensitive and label-free detection. The characteristics make it a potential biosensing system for early recognition that helps the treatment for EV71 infection.

Acknowledgement

歷經兩年的碩士生涯，我學習也體驗到了很多東西，不僅學到實驗所需的技能，也從中加強了提出問題、解決問題等邏輯思考，很感謝我的指導教授楊裕雄老師，提供這麼好的學習及實驗環境，不吝給我指導、幫助和包容。我所研究的論文，希望可以供未來有興趣研究奈米線場效電晶體的同儕做參考，也歡迎大家一起討論研究。

實驗室的氣氛非常和諧，大家也相處得很融洽，沒有拘泥於形式的學長姐學弟妹制度，都親切友善且樂於討論。謝謝實驗室所有的學長姐、學弟妹，不論是酵素組或生電組，謝謝美春學姊細心的帶領新生訓練，之後也教導了很多關於酵素方面的實驗，其實她是一個很風趣的人；謝謝漢平學長總是在歡笑中教導我們；謝謝郁吟學姐、Rich學長，兩位真是學士淵博的人，和他們聊天可以知道很多東西；陸宜學長對實驗的熱忱及豐富的知識也是讓人望塵莫及；小胖雖然一開始講話很難懂，但也很關心我的實驗，提供實驗的方向和設計；小米學姊總是溫柔的和我討論，也辦我度過換題目的那段歲月；普普學長幫我想怎麼合成dopamine-sulfate；最感謝程允學長，教導所有電子相關的知識及想法，在我最後衝實驗的時候還幫我想可以怎麼解決實驗上所遇到的問題；淵仁學長也是，也總是提供我意見；政哲學長常不斷分享他人生的理念，也讓我學到不少；小志學長當實驗的前鋒，省去不少的摸索；秀華學姐也幫了很多；謝謝咏馨在我剛進實驗室好心的待我去搭車，還介紹了分生給我這個外行人聽，靠她講解的分生，是進入這個實驗室一個很重要的起頭；謝謝欣怡，因為有她在實驗室，才讓我覺得不孤單；sonia很辛苦的幫我問關於補助錢的事，一直被我騷擾；謝謝實驗室所有的學長姐和活潑的學弟妹們，讓我在實驗室最後的歲月過的這麼開心，很開心能夠認識你們所有的人，希望大家實驗可以很順利、發很多paper，可以順利如期的畢業，找到好工作，前程似錦。

最後感謝我的爸媽、我的家人他們是我支持下去的原動力，謝謝你們在背後默默的支持我，讓我感動不已。

我會好好規畫我未來的路，人生不能一直活在後悔當中。

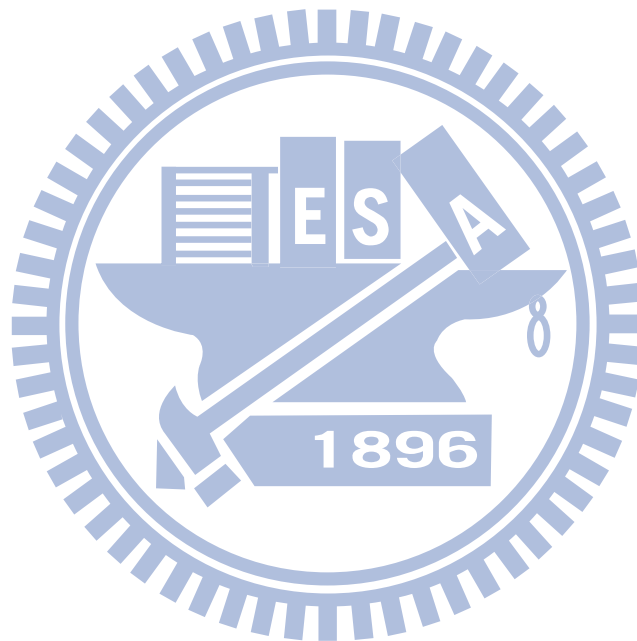
Contents

Abstract (Chinese)	i
Abstract (English)	ii
Acknowledgement	iii
Contents	iv
Contents of Tables	vi
Contents of Figures	vii
Abbreviations	ix
I.	Literatures review.....	1
1.1	Enterovirus.....	1
1.1.1	An introduction to enterovirus.....	1
1.1.2	Mode of transmission.....	2
1.1.3	Pathogenesis.....	2
1.1.4	Epidemiology.....	4
1.1.5	Conventional clinical diagnosis.....	7
1.2	Polysilicon nanowire field-effect transistor (poly SiNW-FET)	10
1.2.1	Introduction of SiNW.....	10
1.2.2	Applications of poly SiNW-FET to biomedical sensing.....	11
1.3	Commercialize products.....	13
1.3.1	DR. EV IVD Kit (晶宇- 腸病毒體外診斷試劑套組).....	13
II	Materials and Methods.....	14
2.1	Fabrication of poly SiNW-FET devices.....	14
2.2	Immobilization of captured DNA probe on poly SiNW-FET...	14

2.2.1	Materials	14
2.2.2	Equipments.....	18
2.2.3	Functionalized poly SiNW-FET with capture DNA probe.....	19
2.3	Microfluidic system integrated with poly SiNW-FET.....	21
2.3.1	Preparation of microfluidic channel with PDMS.....	21
2.3.2	Poly SiNW-FET integrated with microfluidic system.....	21
2.4	Electric measurements of poly SiNW-FET.....	23
2.4.1	The measurement of I_D - V_G curves.....	23
2.4.2	The measurement of I_D -time curves.....	24
III	Results and Discussion	25
3.1	To confirm the immobilization step with target DNA labeled FAM.....	25
3.2	Electronic responses from specific DNA/DNA interaction on poly SiNW-FET.....	28
3.2.1	NW immobilized with EV71 _{capture} DNA probe and I_D - V_G curve was obtained with micro pipette.....	28
3.2.2	NW immobilized with EV71 _{capture} DNA probe and I_D -time curve was obtained with microfluidic system.....	32
3.2.3	NW immobilized with CA16 _{capture} DNA probe and I_D -time curve was obtained with microfluidic system.....	36
3.2.4	Concentration-dependent electric response of EV71 _{capture} functionalized poly-SiNW FET device.....	40
IV	Summary and perspective.....	43
V	References.....	44
Appendix I	DNA Immobilize to the Nanowire Surface.....	51

Contents of Tables

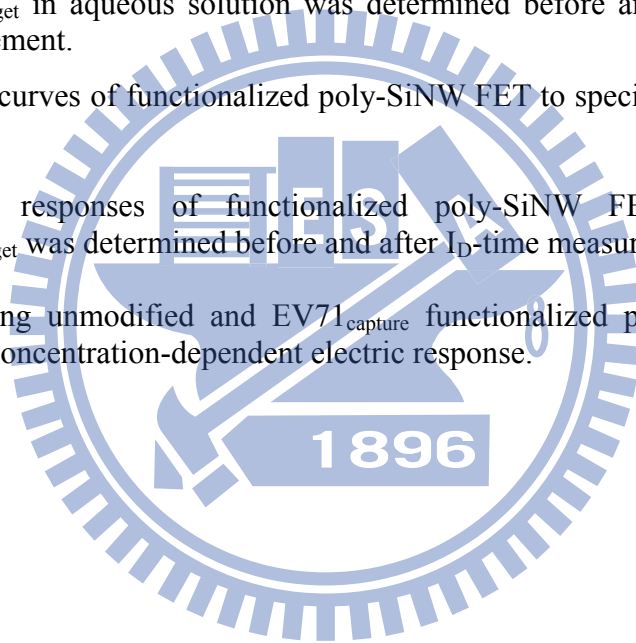
Table 1	Enterovirus were classified based on their genomic sequences.....	1
Table 2	Proposed pathogenesis of severe Enterovirus 71 infections.....	3
Table 3	The common disease related enterovirus serotypes.....	3
Table 4	Historical perspective and case incidences of Enterovirus 71 in worldwide.	5
Table 5	The detection limit of all kinds of novel sensors.....	12
Table 6	Compare the advantages and drawbacks of poly SiNW-FET and traditional clinical diagnosis.....	13



Contents of Figures

Figure 1	The epidemiology of enterovirus around the world, since 1969.	5
Figure 2	Epidemic situation of Enterovirus infection with severe complications in Taiwan, 1998-2008	6
Figure 3	The distribution of serotypes of virus isolation from severe fatal case, 1998~2006	6
Figure 4	Comparison of time of clinical diagnosis and Enterovirus life cycle in host is related to transmission speed.	9
Figure 5	Schematic diagram of DNA probe immobilization	20
Figure 6	The microfluidic channel are used for the biosensing with poly SiNW-FET	22
Figure 7	The apparatus for electric measurement	22
Figure 8	Fluorescence microscopic image of the unmodified EV71 capture DNA probe with poly SiNW-FET device following reaction with 5-FAM dye.	26
Figure 9	Fluorescence microscopic image was observed EV71 capture DNA probe immobilized on the silicon oxide surface in the absence of glutaraldehyde.	26
Figure 10	Fluorescence microscopic image was observed the device functionalized with specific EV71 capture DNA probe gave the expected fluorescence image.	27
Figure 11	I_D - V_G curve illustrating n-type behavior of poly SiNW-FET after functionalization.	30
Figure 12	The I_D - V_D curves for varying V_G from 0 to 5V at $\Delta V = 1V$	30
Figure 13	Electric responses of functionalized poly-SiNW FET to specific EV71 _{target} in aqueous solution.	31
Figure 14	Concentration-dependent electric response of EV71 _{capture} functionalized poly-SiNW FET device following by EV71 _{target} .	31
Figure 15	Electric responses of functionalized poly-SiNW FET to specific EV71 _{target} in aqueous solution was determined before and after I_D -time measurement.	33

Figure 16	I_D -time curves of functionalized poly-SiNW FET to specific EV71 _{target} in PBS.	33
Figure 17	Electric responses of functionalized poly-SiNW FET to specific EV71 _{target} in aqueous solution was determined before and after I_D -time measurement.	34
Figure 18	I_D -time curves of functionalized poly-SiNW FET to specific EV71 _{target} in PBS.	35
Figure 19	Electric responses of functionalized poly-SiNW FET to specific CA16 _{target} in aqueous solution was determined before and after I_D -time measurement	37
Figure 20	I_D -time curves of functionalized poly-SiNW FET to specific CA16 _{target} in PBS.	37
Figure 21	Electric responses of functionalized poly-SiNW FET to specific CA16 _{target} in aqueous solution was determined before and after I_D -time measurement.	38
Figure 22	I_D -time curves of functionalized poly-SiNW FET to specific CA16 _{target} in PBS.	39
Figure 23	Electric responses of functionalized poly-SiNW FET to specific EV71 _{target} was determined before and after I_D -time measurement.	41
Figure 24	comparing unmodified and EV71 _{capture} functionalized poly-SiNW FET device concentration-dependent electric response.	42



Abbreviations

EV71: Enterovirus 71

Poly SiNW-FET: poly Silicon nanowire field-effect transistor

CA16: Coxsackievirus 16



I. Literatures review

1.1 Enterovirus

1.1.1 An introduction to enterovirus

The enterovirus belongs to family Picornaviridae, single-strand RNA virus. They consist of poliovirus (PV, 1-3 serotypes), coxsackievirus group A (CA, 1-22, 24 serotypes), group B (CB, 1-6 serotypes), and echovirus (EV, 1-33 serotypes, except 8, 10, 28) [1]. Since the 1960s, 4 newer enteroviruses have been discovered and named with serial number only, such as enterovirus 68-71 [2, 3]. Since 2000, enteroviruses were classified by genomic sequencing to human poliovirus and human enteroviruses A to D [4] (Table 1). The major outbreak occurred in Taiwan in the summer of 1998 is Enterovirus 71 [5].

Table 1 Enterovirus were classified based on their genomic sequences

Classified	Serotypes
Human enterovirus A (HEV-A)	Coxsackievirus A2-8, 10, 12, 14, 16 Enterovirus 71, 76, 89-92
Human enterovirus B (HEV-B)	Coxsackievirus A9 Coxsackievirus B1-6 Echovirus 1-7, 9, 11-21, 24-27, 29-33 Enterovirus 69, 73-75, 77-88, 93, 97-98, 100-101
Human enterovirus C (HEV-C)	Coxsackievirus A1, 11(15), 13(18), 17, 19-22, 24 Enterovirus 95-96, 99, 102 Poliovirus 1-3
Human enterovirus D (HEV-D)	Enterovirus 68, 70, 94
New (unclassified)	

Enterovirus 71 (EV71) belongs to human enterovirus A (HEV-A). EV71 was further classified by their nucleotide sequence to genotype A, B, and C. Genotype B could be further classified into subtypes B1 to B5; and genotypes C into subtypes C1 to C5 [6, 7]. EV71 and coxsackievirus group A16 (CA 16) are similar very much and both cause hand-foot-mouth disease (HFMD). However, EV71 associated with the further development of acute neurological disease, including poliomyelitis-like paralysis, encephalitis, and aseptic meningitis. The primary agent in fatal case was EV71 which defined by the endemic in Taiwan in 1998 [3].

1.1.2 Mode of transmission

Enterovirus infection occurs worldwide. Human is the only known natural host for enterovirus. EV71 is primarily transmitted through the fecal-oral route. Respiratory droplets are another route of transmission. Enteroviruses have been detected in water, soil, vegetables and shellfish and may possibly be transmitted in the community by contact with contaminated food or water. By Dr. Chang LY's research during the 1998 epidemic, the isolation rate of throat swabs was higher than rectal swabs. EV71 could survive 1-2 weeks in the pharynx and 6-8 weeks in feces. It suggest that during the acute phase of disease, the respiratory droplets or saliva of patients are highly contagious and indicates that in limiting the spread of the epidemic, the respiratory isolation of HFMD patients could be important [8].

1.1.3 Pathogenesis

Clinically, it's difficult to distinguish the specific cause of most enterovirus infection. Most enterovirus infection usually develops no clinical symptoms, mild upper respiratory symptoms, a flu-like illness with fever, or self-limited infections,

like Hand-foot-and-mouth disease (HFMD) and herpangina. But some may develop severe neurologic disease or die, especially in young children[3]. After the incubation period ranges from 2-10 days, usual duration of illness is 3 to 6 days, symptoms start with fever and general malaise[9]. After morbidity, its rapid deterioration within average 3 days, and the majority of EV71 infected with severe complications are myoclonic jerks, hyperglycemia, encephalomyelitis and cardiopulmonary failure...etc [3, 5, 10].

Table 2 Proposed pathogenesis of severe Enterovirus 71 infections [3]

Stage	Syndrome	Underlying cause
1	Hand-foot-and-mouth disease (HFMD)/ herpangina	-
2	Encephalomyelitis	Direct invasion or viremia
3	Cardiopulmonary failure A: Hypertension B: Hypotension	Neurogenic inflammatory response
4	Convalescence	-

Table 3 The common disease related enterovirus serotypes[11].

Common diseases	Virus serotype
hand-foot-mouth disease (HFMD)	Coxsackievirus group A16 (CA16), CA4, 5, 9, 10, CB2, 5, EV71
Herpangina	CA 1-10, CA16, CA22, EV71
Pleurodynia	Coxsackievirus group B (CB)
Acute myocarditis and pericarditis	CB
Acute meningitis and encephalitis	CA10
Aseptic meningitis and encephalitis	Coxsackievirus, poliovirus, echovirus, EV71
Febrile illness with rash	Coxsackievirus, echovirus

1.1.4 Epidemiology

Young children are most susceptible to EV infection. Males more often develop clinically-recognizable disease than females [12].

Enterovirus 71 was first isolated from the stool of an infant with aseptic meningitis in California in the United States in 1969 [13]. Since then, EV 71 has been identified in many parts of the world. Two patterns of EV 71 outbreak have been classified. Small outbreaks involve with occasional patient death, this occurred in the United States, Australia, Sweden, and Japan [14-17]. The other severe outbreaks associated with high mortality, which occurred in Bulgaria in 1975 with 44 deaths [18], in Hungary in 1978 with 45 deaths [19], in Malaysia with at least 30 deaths [20], and in Taiwan in 1998 with 78 deaths [21], in 2000 with 25 deaths, in 2001 with 26 deaths [3]. Outbreaks of aseptic meningitis associated with enterovirus infection have been reported from Cyprus in 1996 and Gaza strip in 1997 [22]. Table 4 and Fig. 1 showed the historical perspective and case incidences worldwide [3, 18, 19].

To sort the incidence and case-fatality rate of enterovirus infection from 1998 to 2008 in Taiwan show in Fig. 2.

Table 4 Historical perspective and case incidences of Enterovirus 71 in worldwide.

Year	Description
1969	First isolated in California
1972	Melbourne, Australia
1974	Sweden
1973	Japan
1975	Bulgaria with 44 deaths
1978	Hungary with 45 deaths Japan
1985	Hong Kong
1986	Nan-ao, Taiwan
1997	Malaysia with at least 30 deaths
1998	Taiwan with 78 deaths
2000	Taiwan with 25 deaths
2001	Taiwan with 26 deaths

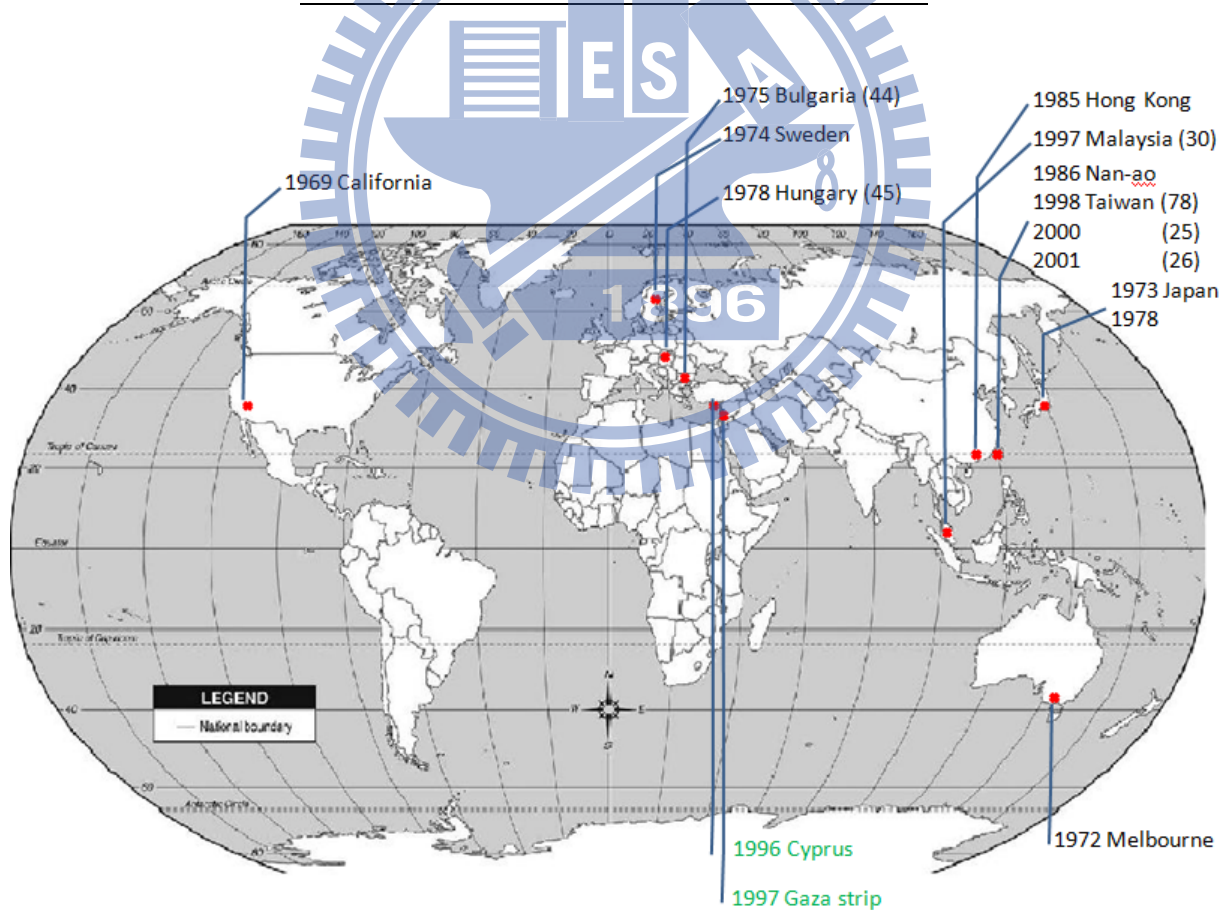


Figure 1 The epidemiology of enterovirus around the world, since 1969.

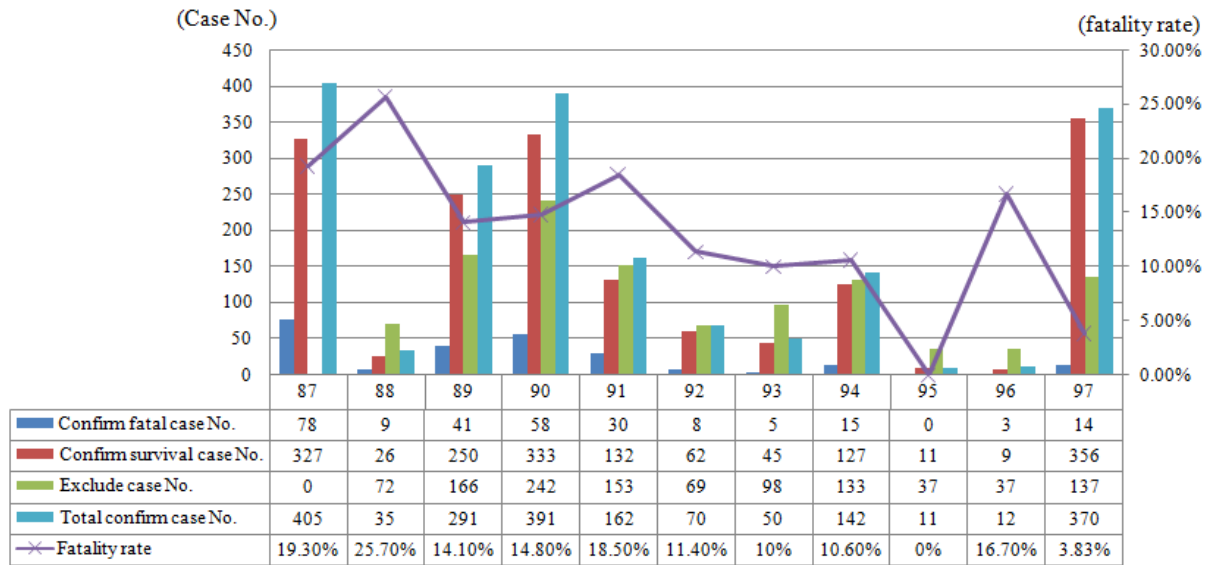


Figure 2 Epidemic situation of Enterovirus infection with severe complications in Taiwan, 1998-2008. (redraw from CDC, 疫情報導 676, 938)

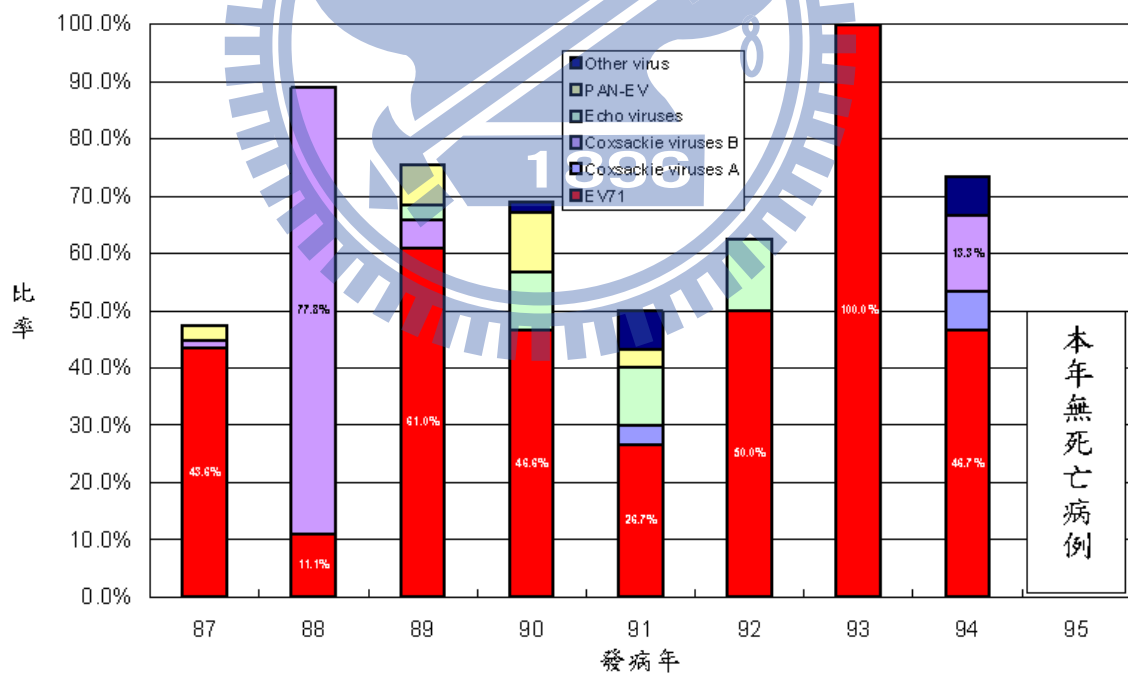


Figure 3 The distribution of serotypes of virus isolation from severe fatal case, 1998~2006 [11]

1.1.5 Conventional clinical diagnosis

The traditional “gold standard” for the diagnosis of Enterovirus infection is virus isolation from clinical specimens in cell culture, followed by serotype identification by neutralization test (NT) and detection of specific enterovirus serotype by the indirect immunofluorescence assay (IFA) [23-25]. The final identification was carried out using a number of different molecular approaches, including reverse transcription polymerase chain reaction (RT-PCR), restriction fragment length polymorphism (RFLP) analysis, and nucleotide sequence analysis of amplicons from various regions of the genome[23, 25-27].

By classification principles set by CDC, March, 2008 is below:

- Enterovirus isolation in cell culture

Diagnosis is made by detecting virus in throat or fecal samples, or more convincingly, from specimens collected from the affected part of the body, for example, cerebrospinal fluid (CSF), biopsy material, and skin lesions. A monkey cell line (LLC-MK2), human lung cell line (MRC-5), human rhabdomyosarcoma cell line (RD), African green monkey kidney cell line (Vero), human lung carcinoma cell line (A549), and human epidermoid carcinoma cell line (Hep-2) were used to grow viruses [23, 25]. Preliminary identification is based on the appearance of a minimum of 14 days for characteristic of a viral cytopathic effect (CPE)[28, 29].

- Enterovirus antisera neutralization test (NT)

Serotype identification was performed by neutralization using Lim Benyesh-Melnick (LBM) pools of types-specific antisera. The serum specimen was diluted by PBS, mixed well, and the mixtures were heated. Then the method

of gold standard procedure was followed to make a two-fold serial dilution out of the sample, and a definite amount (100 CCID₅₀ / 50 μ l) of virus was added to each of diluted solutions. The mixture was then incubated 4 days before its neutralization antibody titer determined [25, 30, 31]. At least a four-fold rise in the level of neutralization antibody titer in serum collected during the acute and convalescent phase of illness, which provides the best evidence of a recent infection[2].

- Immunofluorescence assay (IFA)

When cytopathic effect was observed, infected cells were scraped off the vessels, washed in PBS, spotted on the slides. The monoclonal antibody blends were directly applied to specific wells on each slide. The slides were incubated with a prestandardized dilution of anti-mouse immunoglobulin G fluorescence-conjugated antibody. After mounting, slides were then examined under a fluorescence microscope [23-25]. In Rignonan's research, the sensitivity of the IFA was 73% for polioviruses, 85% for coxsackieviruses type B, and 94% for echoviruses. Specificity was near 100% for polioviruses and coxsackieviruses type B and 94% for echoviruses[24].

- Reverse transcription polymerase chain reaction (RT-PCR)

After RNA extraction, the purity and concentration of RNA was determined both measuring OD at A260/280 and by quantitating the ethidium-stained agarose gel bands. RT-PCR were carried out by RT-PCR beads. The beads contained recombinant Moloney Murine Leukemia virus (M-MuLV) reverse transcriptase for cDNA synthesis, Taq DNA polymerase for amplification, RNase inhibitor,

buffer, dNTPs. RT-PCR products were examined by electrophoresis through 1~3% agarose gels and ethidium bromide staining. The bands migrating at the predicted size were excised and purified for further sequencing analysis [23, 25, 32].

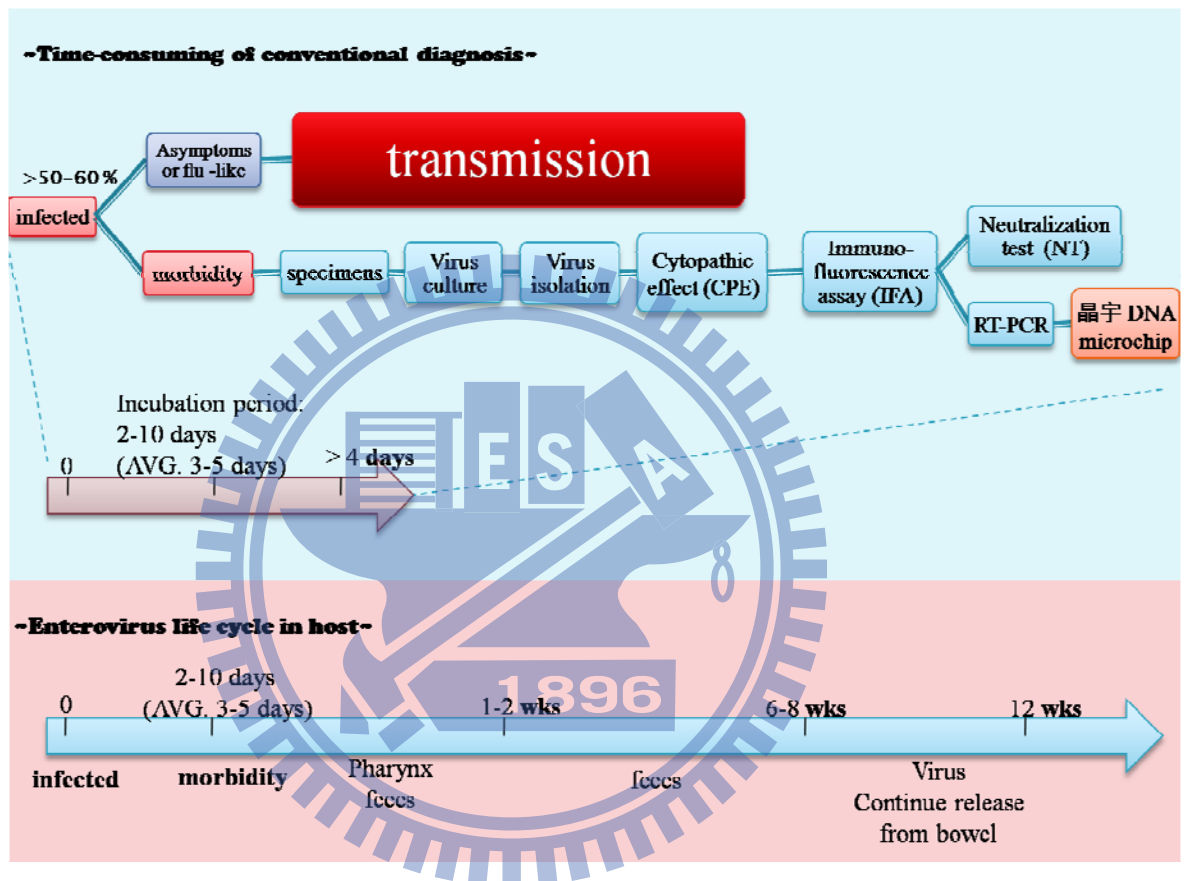


Figure 4 Comparison of time of clinical diagnosis and Enterovirus life cycle in host is related to transmission speed.

These methods often require a relatively high level of sample manipulation that isn't convenient for infection materials. The ability to detect rapidly, directly, and selectively individual virus particles has the potential to significantly impact health care, since it could enable diagnosis at the earliest stages of replication within a host system. We currently lack a sensitive method of diagnosing enterovirus early.

1.2 Polysilicon nanowire field-effect transistor (poly SiNW-FET)

1.2.1 Introduction of SiNW

There are two common ways to fabricate silicon nanowires. Chemical vapor deposition (CVD) method was used to fabricate silicon nanowires by using metal nanoclusters and silane (SiH_4) as the vapor phase reactant. The most famous group is led by Charles M. Liber in Harvard University. Their research focused on was about how to control the growth rate and electrical properties of the carbon nanotube and silicon nanowire was published in Nature in 2000[33]. Then they reported that they can fabricate silicon nanowire field effect transistor in Science in 2001 [34] and they claimed the application of their silicon nanowire field effect transistor which can be used as pH sensor and biosensor , which also published in Science in the same year[35]. They used APTES to modify the surface of the silicon nanowire to improve the performance for pH values sensing and used the biotin to functionalize the surface of silicon nanowire to detect the streptavidin. Furthermore, they announced many researches in many famous internal journals, such as detection of DNA and DNA sequence variations [36], detection of single viruses [37], multiplexed electrical detection of cancer markers and detection to at least 9pg/ml [38], and detection, stimulation, and inhibition of neuronal signals [39]. Charles M. Liber et al. prove that silicon nanowire field effect transistor can not only measure but also detect many kinds of targets. It is worth studying that the silicon nanowire field effect transistor has the capability as a sensor. However, the electrodes of the silicon nanowires which are fabricated by CVD method are arranged difficultly. In order to overcome this obstacle, some groups tried to use e-beam lithography to define nanowire pattern on silicon on insulator (SOI) substrate [40, 41]. Although the width of the silicon nanowire is wider than that fabricated by CVD, it showed good performance of pH values and

proteins detections, for instance, Eric Stern used the biotin to functionalizing the silicon nanowire to detect streptavidin and avidin and can detect at least 10fM. Moreover it can detect to at least 100fM in immunoassay [42].

This kind of fabrication method is easy to arrange the electrodes of the silicon nanowire and to suit the standard CMOS fabrication process. So the difficulty of the fabrication process is minimized. Nevertheless, the cost of the SOI is much higher than silicon wafer to increase the prime cost of the developed sensors.

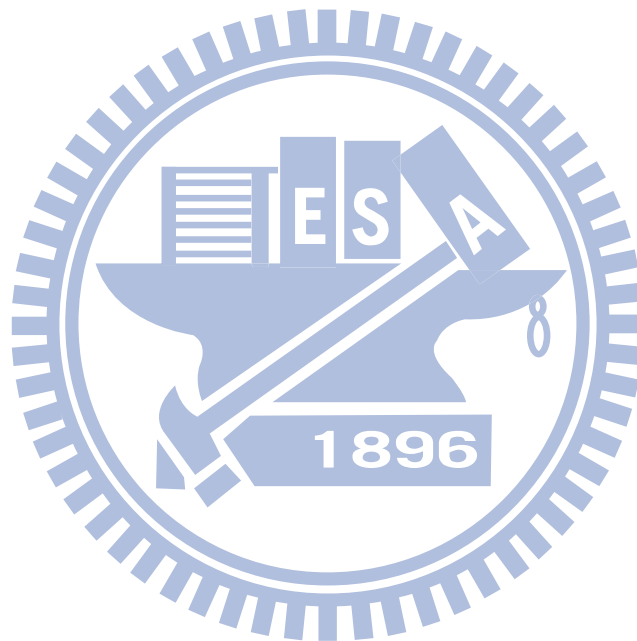
1.2.2 Applications of poly SiNW-FET to biomedical sensing

Conventional techniques for the detection of biomolecular interactions are limited by the need for exogenous labels, time- and labor-intensive protocols, as well as by poor sensitivity performance levels[35]. Material scientists and engineers have progressively miniaturized the materials with advanced CMOS fabrication process that constitute the building blocks of various biomedical devices, such as carbon nanotubes[43], surface plasma resonances (SPR)[44], cantilever[45], quartz crystal microbalance (QCM)[46], and quantum dots[47]. Some of these sensing devices, such as those based on cantilevers and quantum dots, are highly specific, ultrasensitive, and have a short response. However, these devices require integration with optical components in order to translate phenomena on sample surface into a readable signal. The requirement for detection optics is expected to significantly increase the cost of operation for such a device. This progressive downscaling has led to the creation of materials with at least one critical dimension less than the scale of approximately 100 nm. Table 5 compared the relative methods of biosensing, NW-FET can be developed to a highly sensitive, label-free, and real-time biosensor. In the present method, NW-FET has the highest sensitivity, and many research teams consider it as an

important study direction.

Table 5 The detection limit of all kinds of novel sensors.

Transducers	Target	Sensitivity
SPR[44]	Tumor antigen	10-100 pg/ml
Microcantilever [45]	PSA	0.2 ng/ml
QCM[46]	Human-IgG	100 pg/ml
Electrode [48]	IgG	7 pg/ml
SNW-FET[38]	PSA	50-100 fg/ml



1.3 Commercialize products

1.3.1 DR. EV IVD Kit (晶宇- 腸病毒體外診斷試劑套組) [49]

The novel approach is based on hybridization of amplified DNA specimens with oligonucleotide DNA probes immobilized on a microchip. Two oligonucleotides were used as detection probe, the pan-enterovirus located in the 5'-noncoding region (5'-NCR) and the EV71-specific sequence located in the VP2 region. The diagnostic procedure takes 6 hr, exclude specimens pretreatment, such as virus isolation, PCR amplification...etc. The experiment result is presented by colorimetry. All of the specimens identified as enterovirus by viral cultures and IFA using a pan-enterovirus antibody were tested using this microchip. The sensitivity is 89.6 % and its specificity is 90.9 %.

Table 6 Compare the advantages and drawbacks of poly SiNW-FET and traditional clinical diagnosis.

	Chip		Clinical diagnosis		
	NW-FET[50]	DNA microarray chip [49]	IFA[24]	NT[24]	RT-PCR[27]
Accuracy	V	89.6 %	73~94 %		92 %
Label-free	V	Colorimetric	Fluorescence		Fluorescence
Real-time	V	X	X	X	X
Fabrication	V	X	X	X	X
Cost-down	V	400000 /system	X	X	V
Without training	V	X	X	X	X

Define “V” as yes, and “X” as no.

II. Materials and methods

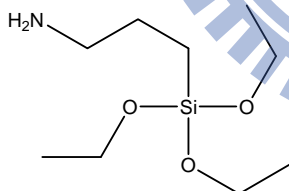
2.1 Fabrication of poly SiNW-FET devices

Poly SiNW-FET devices were fabricated at the National Nano Device Laboratories (Hsinchu, Taiwan) according to previously reported procedures with some modifications to reduce the current leakage in aqueous solution[51]. N-type devices with two poly SiNW channels, 80 nm width and 2 μm length, were fabricated based on poly-silicon sidewall spacer technique. This approach was compatible with current commercial semiconductor process [50, 52-55].

2.2 Immobilization of captured DNA probe on poly SiNW-FET

2.2.1 Materials

1. 3-Aminopropyltriethoxysilane (APTES): $\text{H}_2\text{N}(\text{CH}_2)_3\text{Si}(\text{OC}_2\text{H}_5)_3$



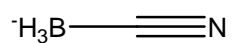
Company: Sigma-Aldrich (USA) (A3648)

CAS Number : 919-30-2

Assay: $\geq 98\%$

2. Sodium cyanoborohydride: NaBH_3CN

Na^+

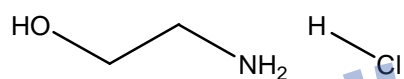


Company: Sigma-Aldrich (USA) (71435)

CAS Number : 25895-60-7

Assay: $\geq 95\%$ (RT)

3. Ethanolamine hydrochloride: $\text{NH}_2\text{CH}_2\text{CH}_2\text{OH} \cdot \text{HCl}$

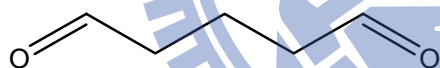


Company: Sigma-Aldrich (USA) (E6133)

CAS Number : 2002-24-6

Assay: $\geq 99\%$

4. Glutaraldehyde solution: $\text{OHC}(\text{CH}_2)_3\text{CHO}$



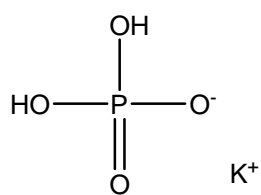
Company: Fluka (USA)

CAS Number : 111-30-8

Grade: technical

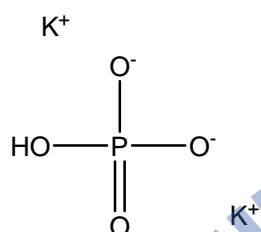
Concentration: $\sim 25\%$ in H_2O (2.6M)

5. Potassium phosphate monobasic: KH_2PO_4



Company: J.T.Baker (USA)

6. potassium phosphate dibasic: K_2HPO_4

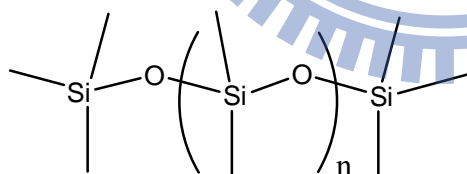


Company: J.T.Baker (USA)

7. Ethanol (99.5%): CH_3OH

Company: Echo Chemical Co. (Taiwan)

8. Polydimethylsiloxane (PDMS): $(\text{H}_3\text{C})_3\text{SiO}[\text{Si}(\text{CH}_3)_2\text{O}]_n\text{Si}(\text{CH}_3)_3$



Company: Sil-More (Taiwan)

9. EV71 DNA sequences were designed for capture probe and the target DNA used on this project are listed as below and based on previous publication [27]. All synthetic oligonucleotides were purchased from MDBio Inc. (Taiwan).

5'-amino C₆ modified captured DNA probe

5'-6 – Carboxyfluorescein (FAM) modified EV71 target DNA

DNA sequences (5'-3')	
5'-H ₂ N C ₆ modified captured DNA probe	Target DNA
EV71 ^a	GTG GCA GAT GTG ATT GAG AG CTC TCA ATC ACA TCT GCC AC
CA16 ^b	GAG TGA TGG TTC AAC ACA CA TGT GTG TTG AAC CAT CAC TC

^a relative to BrCr nt 2448-2467

^b relative to G-10 nt 2666-2685

10. Phosphate buffer solution (PBS) was prepared in deionized water (DIW) and its pH was adjusted to 7.0.

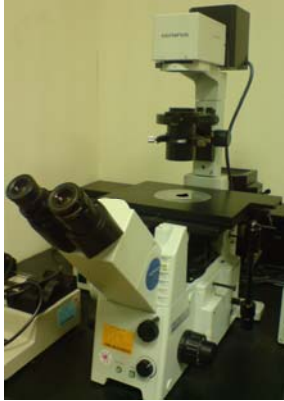
11. Deionized water (DIW)

resistance of water: 18.2 MΩcm

ultra-pure water system (Barnstead).

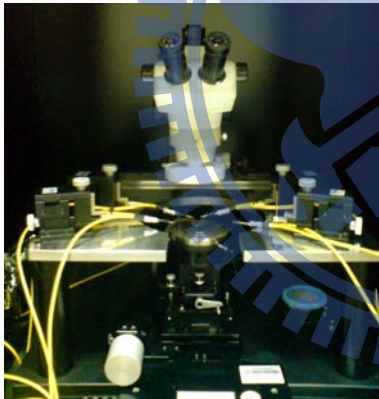
2.2.2 Equipments

1. Fluorescence microscope



Company: Olympus

2. Probe station



Company: Calfa (奕葉)

3. Model 2636 Dual-channel System SourceMeter Instrument (Low Current)



Company: Keithley

2.2.3 Functionalized poly SiNW-FET with capture DNA probe

The microfluidic channel, which was made with acrylic and polydimethylsiloxane (PDMS) was placed on top of the device integrated with metal holder to hold the aqueous solution surrounded poly-SiNW. The poly-SiNWs were firstly washed by ethanol solution to remove contaminants before 2.0% APTES ethanol solution was pumped into the microfluidic channel for 17 min to introduce amino group onto the poly-SiNW surface. The device was then washed with pure ethanol (99.5%) once, and heated at 120 °C for 10 min to remove the surplus ethanol. Secondly, the device surface was covered with 2.5% glutaraldehyde in 10 mM PBS (pH 7.0) and 4 mM sodium cyanoborohydride for 1 hr followed by PBS wash. Finally, the 10 μ M 5'-amniommodified captured DNA probe was coupled to the surface of the nanowire in PBS containing 4 mM sodium cyanoborohydride for 1 hr. The un-reacted aldehyde groups were blocked by mixing with 50 mM ethanolamine for 35 min and the modified poly-SiNW FET was washed with PBS.

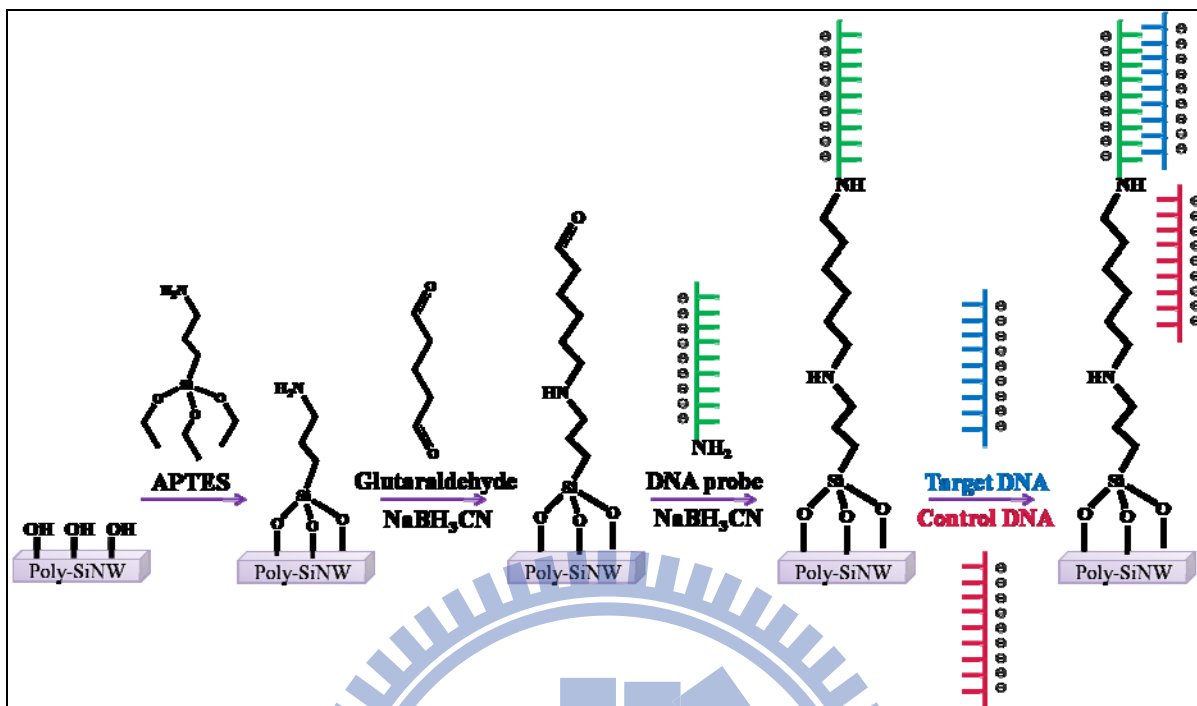
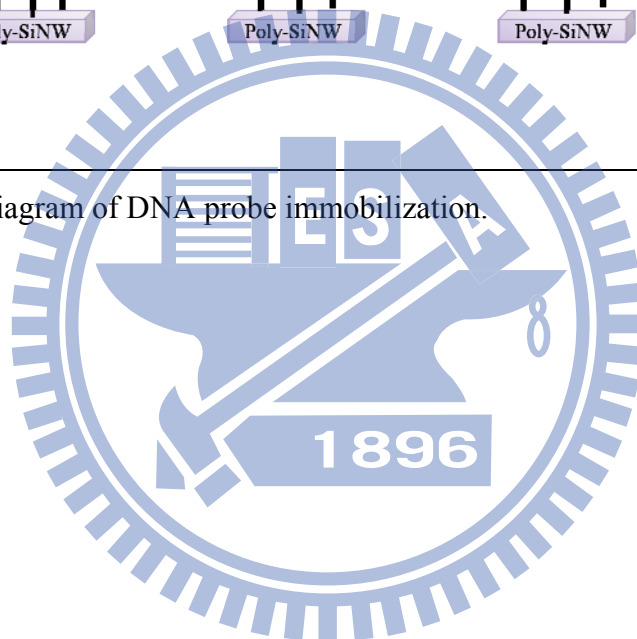


Figure 5 Schematic diagram of DNA probe immobilization.



2.3 Microfluidic system integrated with poly SiNW-FET

2.3.1 Preparation of microfluidic channel with PDMS

To still and mix reagent A and B (gravity ratio A:B = 10:1) well. Use vacuum pump to degas about 30min until most bubbles are gone. Pour it to mother mode (glass). Bake PDMS with oven at 70°C for 30 minutes. Peel PDMS structure off carefully from mother mode. Punch input and output holes. Surface may need to be clean with acetone

2.3.2 Poly SiNW-FET integrated with microfluidic system

Clean PDMS microfluidic channel with acetone to clean the dust and organical particles. Bond PDMS microfluidic channel to nanowire devices. A mechanical gear was designed which uses a limp blanket of acrylic to compress the PDMS structure and to make it stick to the wafer surface (Fig. 6). Backside of the wafer contacts with a stainless steel, allowing a bias applied to the substrate serving as a back gate of the NW devices and could be adjusted in the subthreshold region of the transfer characteristics of the NW device. (Fig. 7)

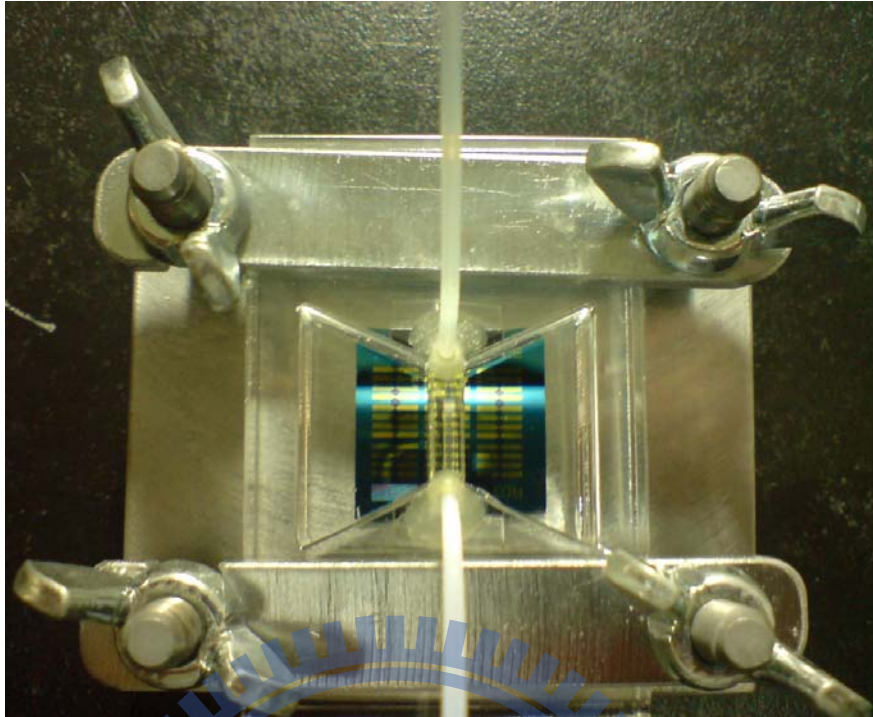


Figure 6 The microfluidic channel are used for the biosensing with poly SiNW-FET

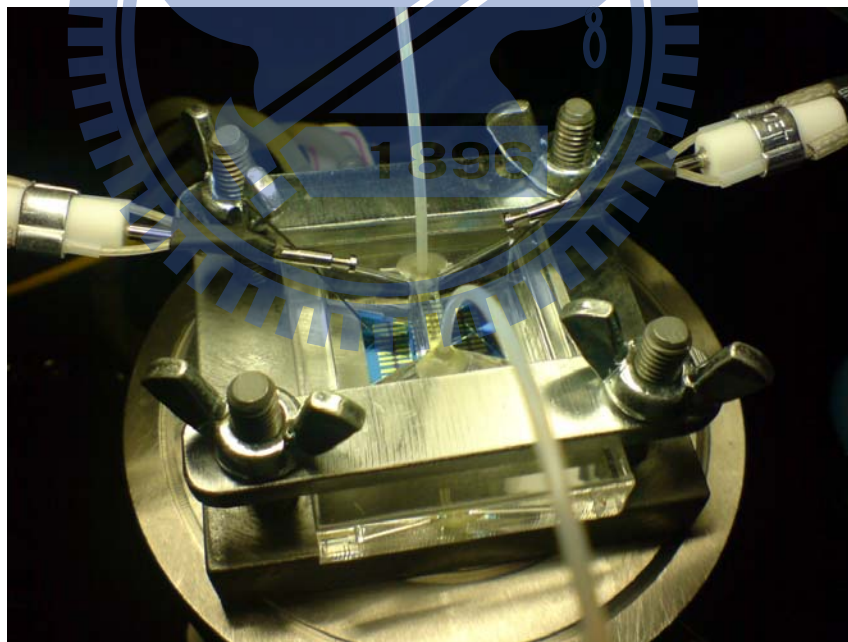


Figure 7 The apparatus for electric measurement.

2.4 Electric measurements of poly SiNW-FET

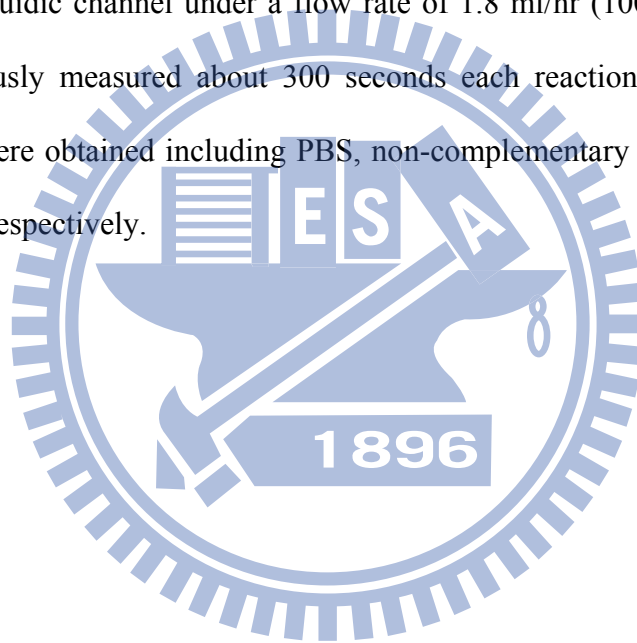
The gate potential and source/drain bias voltage were controlled by chip analyzer (Keithley 2636). Generally, the I_D was measured at several constant bias voltage (V_G from 0 to 3 V with a step of 0.5 V) for the measurement of I_D - V_D curves while sweeping the V_D from 0 to 1.5 V to test the performance of poly SiNW-FET. We divide the biosensing parameters into two electric measurements. They are I_D - V_G measurement and I_D -time measurements:

2.4.1 The measurement of I_D - V_G curves

In the general I_D - V_G curve measurement parameters, the drain current (I_D) was measured at constant bias voltage ($V_D = 0.5V$) while sweeping the gate potential (V_G) from 0 to 1.5 V. We performed a sweep started at 0 V bias. To ensure that the device was in the initial state after the stabilized base I_D - V_G curves was obtained as PBS (10 mM, pH 7.0) was injected, and the EV71 target DNA in PBS (about 0.1 μ l) was load directly on the nanowire device with a micro pipette. When comparing I_D - V_G curve behavior to those controlled experiments, we noted that the biosensing test gave the current shift at the same bias conduction. The electric characteristic of DNA/DNA hybridization was observed as soon as the target DNA was added. It took 30 sec to obtain and I_D - V_G curve and the I_D - V_G curve remained stable during the incubation. In a typical experiment, the determination of I_D - V_G curves was repeated at least 3 times or until it become stable without current shift to make sure that no further variation can be observed.

2.4.2 The measurement of I_D -time curves

After the stabilized base I_D - V_G curves was obtained in PBS (10 mM, pH 7.0), V_G was choose from the linear region that have the largest variation of I_D . Generally, in the I_D -time curve measurement parameters, the I_D was measured at constant bias voltage ($V_D = 0.5$ V) and gate potential each experiments to test the poly SiNW-FET performances in aqueous solution. I_D -time data were recorded while buffer solutions, flowed through the microfluidic channel. DNA sensing experiments were performed in the microfluidic channel under a flow rate of 1.8 ml/hr (100 μ l / 200 sec) in PBS and continuously measured about 300 seconds each reactions. The orders of each experiment were obtained including PBS, non-complementary target DNA, PBS, and target DNA, respectively.



III. Results and Discussion

3.1 To confirm the immobilization step with target DNA labeled FAM

The EV71 DNA functionalized device was monitored by fluorescence labeling using 5'-5-FAM modified EV71 target DNA (5'-5-FAM-EV71 DNA_{target}) as the fluorescence reporter. EV71 capture (EV71_{capture}) DNA probe is a single-strand DNA sequences which is used to recognize the complementary EV71 target (EV71_{target}) DNA. EV71_{capture} DNA probe was functionalized on the surface of poly SiNW-FET according to the procedure diagramed in Fig. 8 Fluorescence was observed with some background on the surface of the device with the addition of 5'-5-FAM-EV71 DNA_{target} on unmodified EV71 capture DNA probe under blue light excitation (Fig. 8). EV71 capture DNA probe cannot be linked to the silicon oxide surface in the absence of glutaraldehyde, and thus the fluorescence was not observed in Fig. 9 either. Clear distinction in fluorescence was observed in Fig. 10. Only the device functionalized with specific EV71 capture DNA probe gave the expected fluorescence upon hybridization with 5'-5-FAM-EV71 DNA_{target} under blue light excitation.

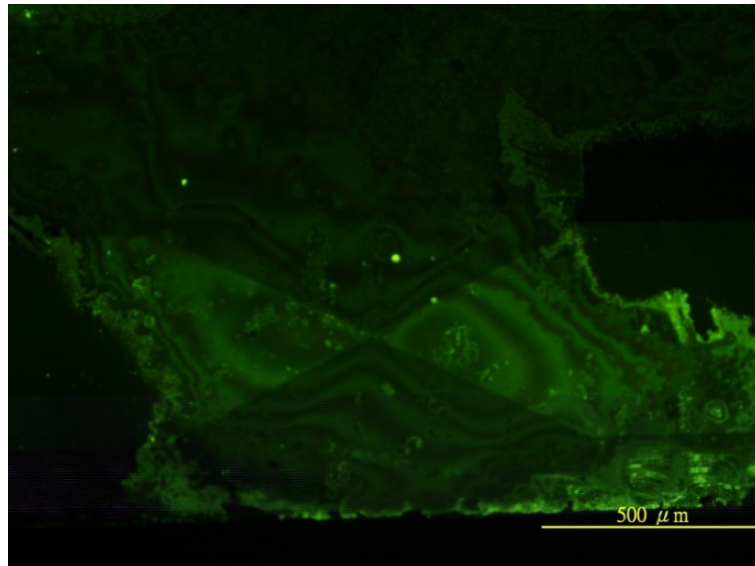


Figure. 8 Fluorescence microscopic image of the unmodified EV71 capture DNA probe with poly SiNW-FET device following reaction with 5-FAM dye.

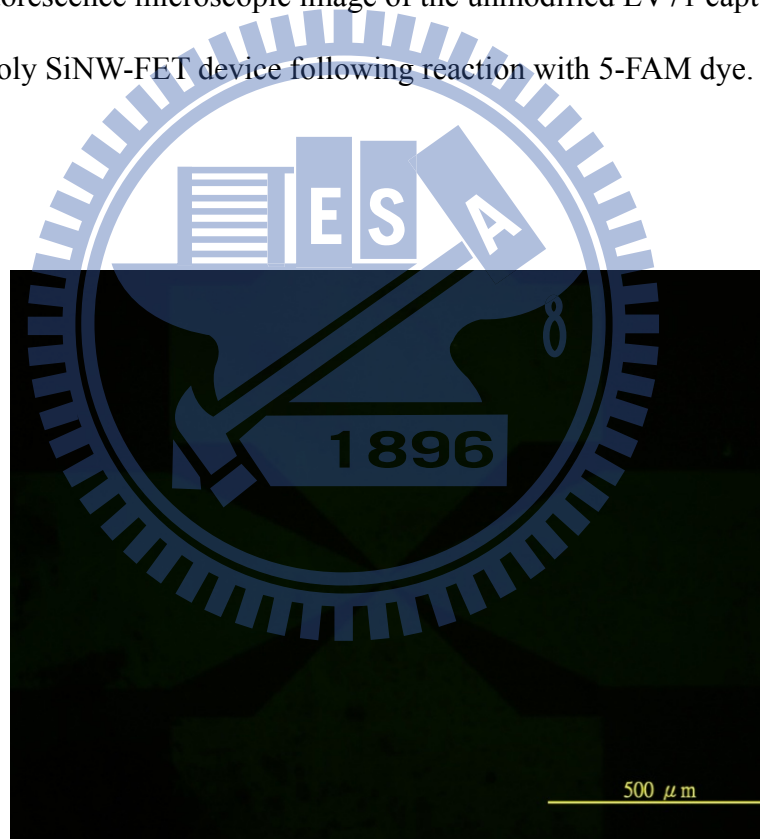


Figure. 9 Fluorescence microscopic image was observed EV71 capture DNA probe immobilized on the silicon oxide surface in the absence of glutaraldehyde.

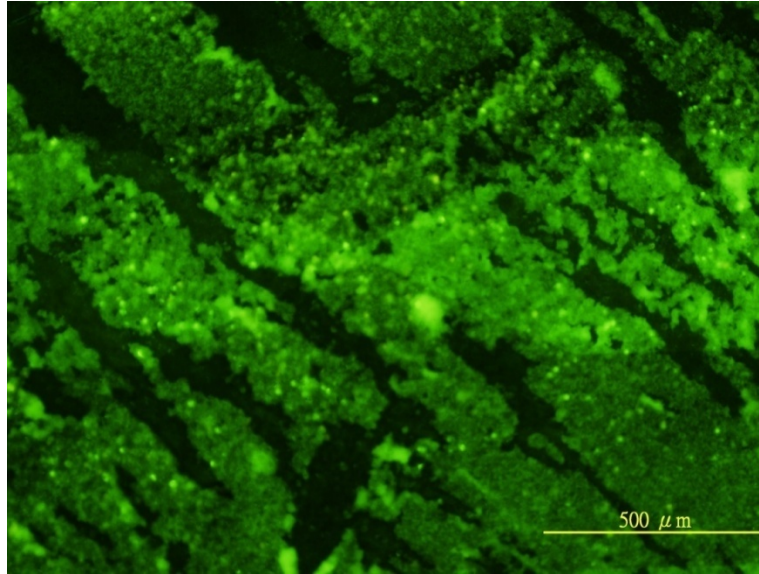
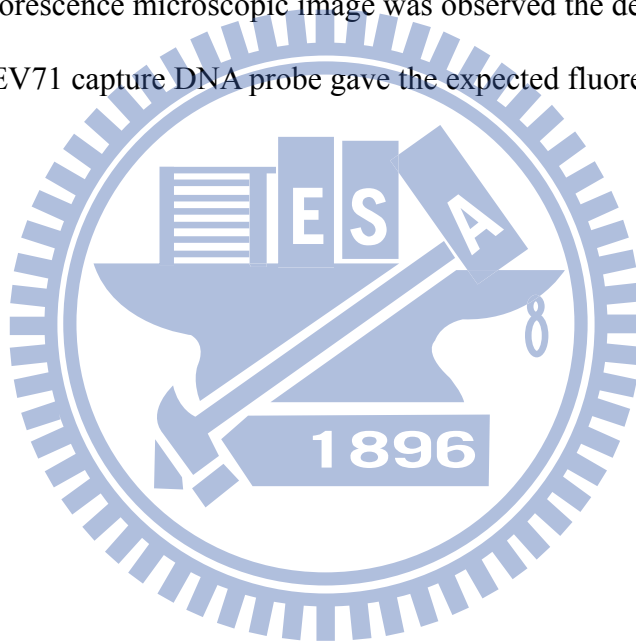


Figure. 10 Fluorescence microscopic image was observed the device functionalized with specific EV71 capture DNA probe gave the expected fluorescence image.



3.2 Electronic responses from specific DNA/DNA interaction on poly SiNW-FET

3.2.1 NW immobilized with EV71_{capture} DNA probe and I_D - V_G curve was obtained with micro pipette

Typical characteristic of poly SiNW-FET at room temperature was shown in Fig. 11 and Fig. 12. The I_D versus V_G (I_D - V_G , from 0 to 2 V) output characteristic of with the constant V_D (0.5 V) exhibited excellent semiconductor FET characteristics, illustrating n-type behavior. A good device performance with high on/off current ratio (around five orders) (Fig. 11). The I_D versus V_D output characteristics of a representative poly SiNW-FET were shown in Fig. 12 for V_G varying from 0 to 5 V with 1 V per step. The measured I_D - V_D characteristics show well-saturated behavior with back-gate controlled. In the linear region, at constant V_D , the current increase with gate potential. The electrical characterization verified that this fabrication approach produced high-performance poly SiNW-FET device.

Sensitivity and specificity of functionalized poly SiNW-FET for biosensing DNA/DNA interactions are shown in Fig. 13 and 14. The increase in negative charges resulted from hybridization between capture DNA probe ($\text{DNA}_{\text{capture}}$) and complementary target DNA ($\text{DNA}_{\text{target}}$) can affect greatly the surface conductivity of SiNW-FET. For an N-type NW-FET, a decrease of the current will be expected when negative charges comes from phosphoric acid of DNA were introduced on sensing surface of n-type device[56]. In Fig. 13 the I_D - V_G curves were obtained in PBS buffer (10mM, pH 7, black square), and following the addition of coxsackievirus A16 (10 pM, red circle) and addition of EV71 (10 pM, blue triangle), respectively. PBS and CA16 about 0.1 μl was load directly on the nanowire device with a micro pipette as controlled experiments and continuously measured until it become stable without

current shift to ensure that no further variation can be observed. The I_D - V_G curves remained unchanged indicated that the electric property of poly SiNW-FET was stable in the presence of non-interacting charged molecules, which may exist in a variety of biological samples. However, when a complementary EV71 target DNA ($EV71_{target}$) hybridized with EV71 capture DNA probe ($EV71_{capture}$), the current decrease was observed.

The lowest detectable concentration and detection range of $EV71_{target}$ with $EV71_{capture}$ modified poly SiNW-FET was further demonstrated electric responses in Fig. 14 A constant V_D was set at 0.5 V for all the electric measurement. The I_D - V_G curves were determined as described above by using different concentrations of $EV71_{target}$. After the base I_D - V_G curve was obtained in PBS buffer, PBS buffer contained $EV71_{target}$ at varied concentrations, respectively, and their I_D - V_G curves were determined. For the $EV71_{capture}$ functionalized poly SiNW-FET, I_D - V_G curves were indistinguishable in PBS and in the presence of $CA16_{target}$. Concentration-dependent electric responses were observed for $EV71_{target}$ concentration increasing from 1 fM to 10 pM. The concentration more increase, the influence on the current smaller was evidences when $EV71_{target}$ concentration is 10 pM. This characteristic further confirmed that change of current in I_D - V_G curve was specifically affected by the interactions between $EV71_{target}$ and $EV71_{capture}$ on the SiNW surface. The I_D - V_G curve become change-less after saturation even much higher concentration of $EV71_{target}$ (10 pM) was added. According to the approximate volume of $EV71_{target}$ used ($0.1 \mu l$), the number of $EV71_{target}$ molecules were about 600 at 1 fM. This number is the same as our research[57]. This research is expected because they are both composed by 20-mer DNA, produces about twenty extra negative charges.

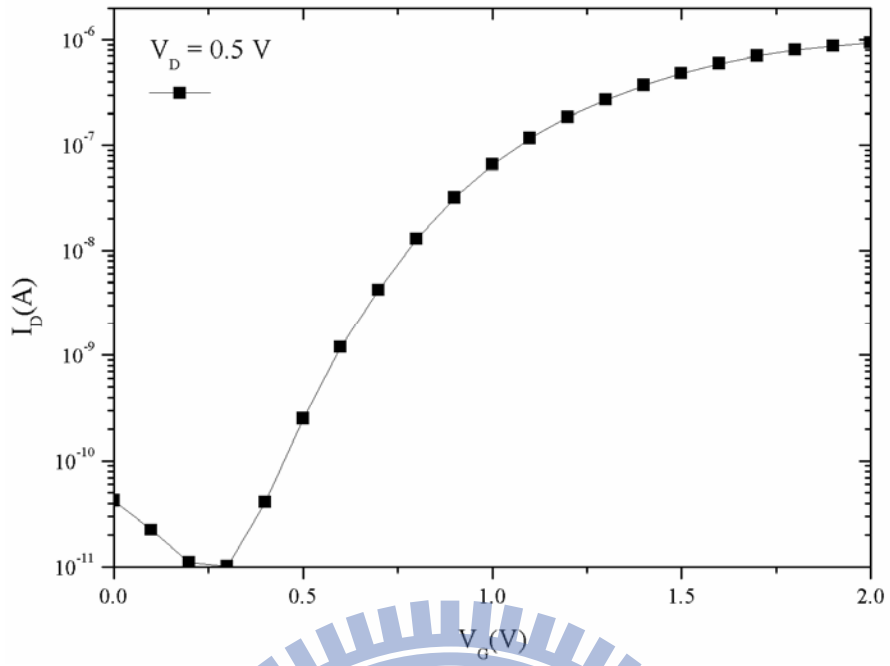


Figure 11 I_D - V_G curve illustrating n-type behavior of poly SiNW-FET after functionalization.

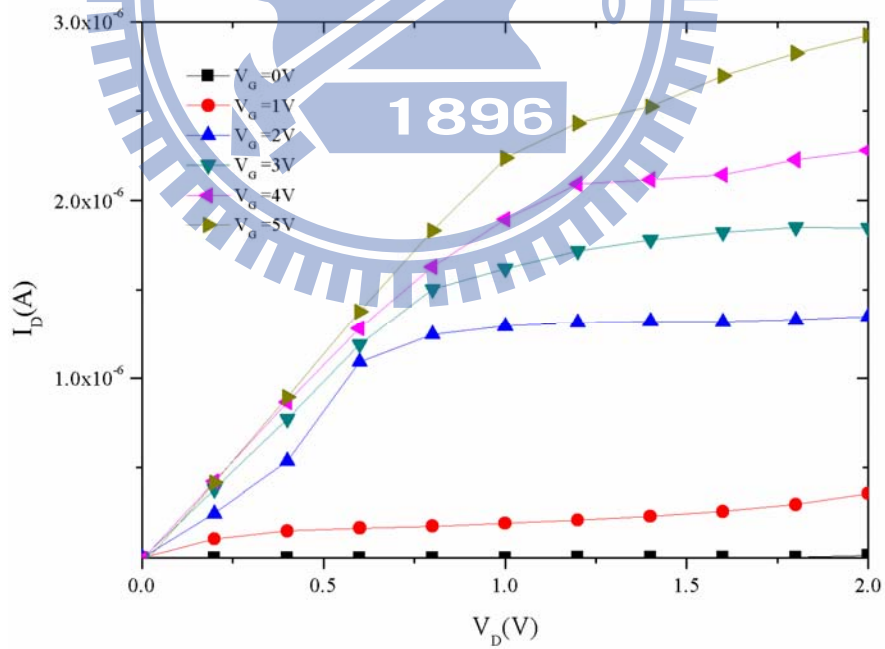


Figure 12 The I_D - V_D curves for varying V_G from 0 to 5V at $\Delta V = 1V$.

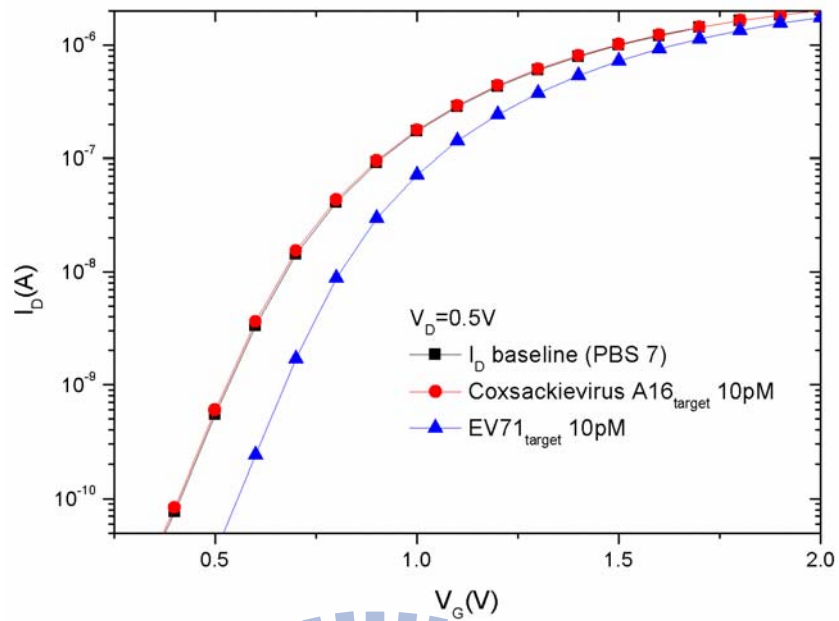


Figure 13 Electric responses of functionalized poly-SiNW FET to specific EV71_{target} in aqueous solution.

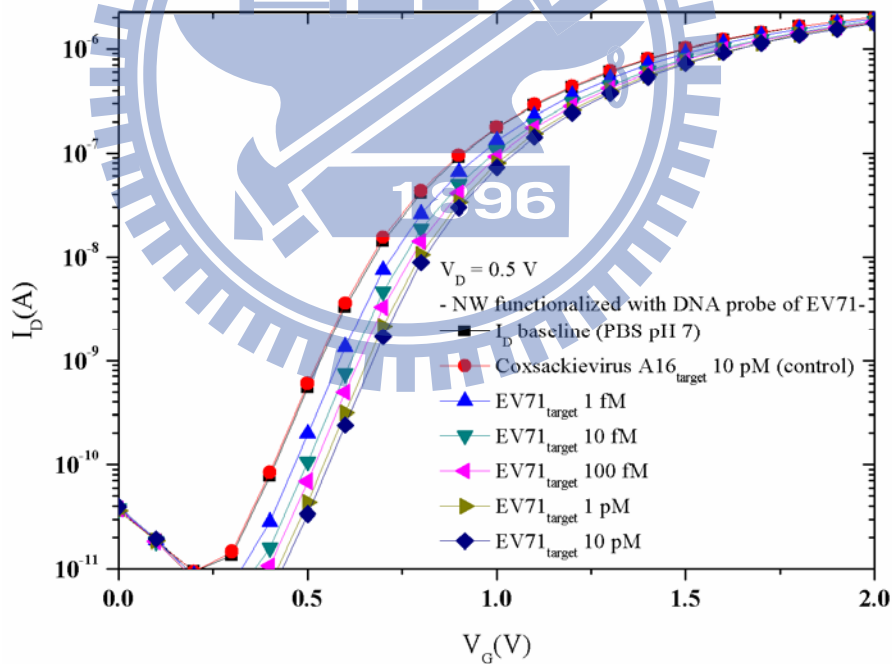


Figure 14 Concentration-dependent electric response of EV71_{capture} functionalized poly-SiNW FET device following by EV71_{target}.

3.2.2 NW immobilized with EV71_{capture} DNA probe and I_D-time curve was obtained with microfluidic system

In Fig. 15 the I_D-V_G curves were obtained in PBS buffer (black square) first. To choose the I_D (about 10⁻⁹) was induced by V_G (0.7 V) in the linear region with great variation and starts to measure the electric response in the PBS buffer as I_D baseline. PBS buffer solution contained CA16_{target} (10 pM) and EV71_{target} (10 pM). PBS buffer, CA16_{target}, PBS, and EV71_{target} were injected into the channel (arrow indicated), respectively, and I_D-time curve was determined (Fig. 16). Adding PBS buffer as controlled experiments and continuously measured until it become stable without current shift to ensure that no further variation can be observed. When the electric response of PBS to surface of device was stable, then adding next flowing reagent and continuously measured about 300 seconds each reaction. When comparing current curve behavior to those controlled experiments, such as non-complementary CA16_{target} DNA and PBS buffer, we noted that the biosensing test gave the current shift is smaller than complementary EV71_{target} DNA hybridized with EV71_{capture} DNA probe, the current decrease was observed. After measuring I_D-time curve, the electric characteristic of the same device was shown in Fig. 15 (red circle). The range of current shift of before and after I_D-time measurement is matched between I_D-V_G curves and I_D-time curve.

To compare the experiment results among Fig. 14, Fig. 15 and Fig. 16, the current shift was observed in Fig. 16. It might be the variation of scale is too small to see the significantly change which was shown in I_D-V_G curves. It proves that the characteristic of each device might be different, so we observed the current shift by time afterward.

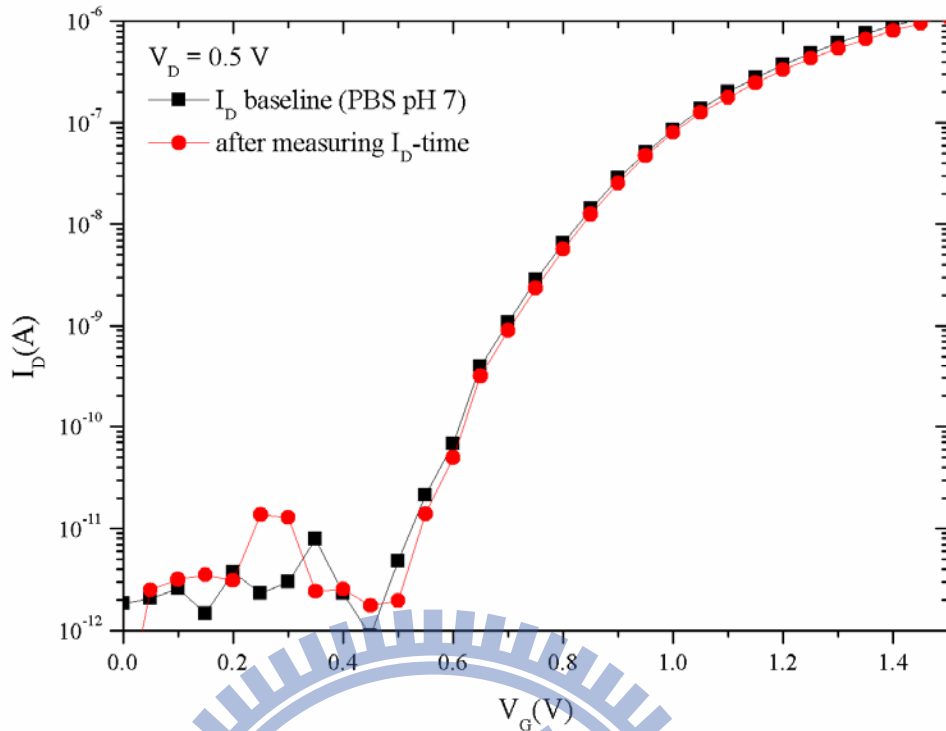


Fig. 15 Electric responses of functionalized poly-SiNW FET to specific EV71_{target} in aqueous solution was determined before and after I_D -time measurement.

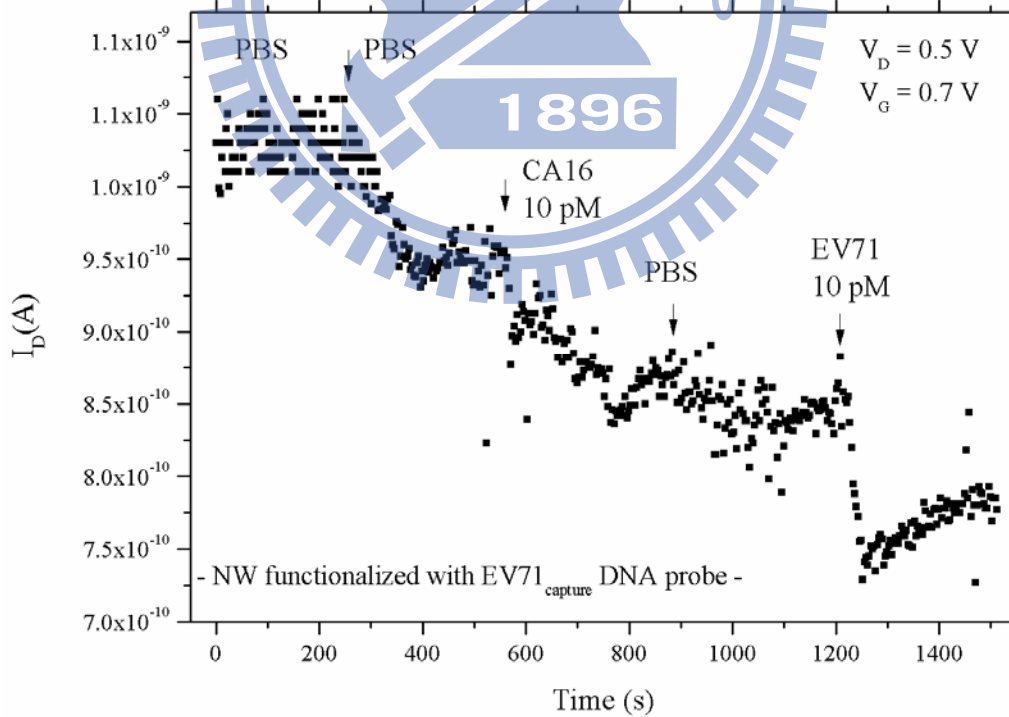


Figure 16 I_D -time curves of functionalized poly-SiNW FET to specific EV71_{target} in PBS.

The experimental method is the same as above and observed the same result which is shown in Fig. 17 and Fig. 18. These two experiments is done in the same die and day. It proves that the experiment is reproducible.

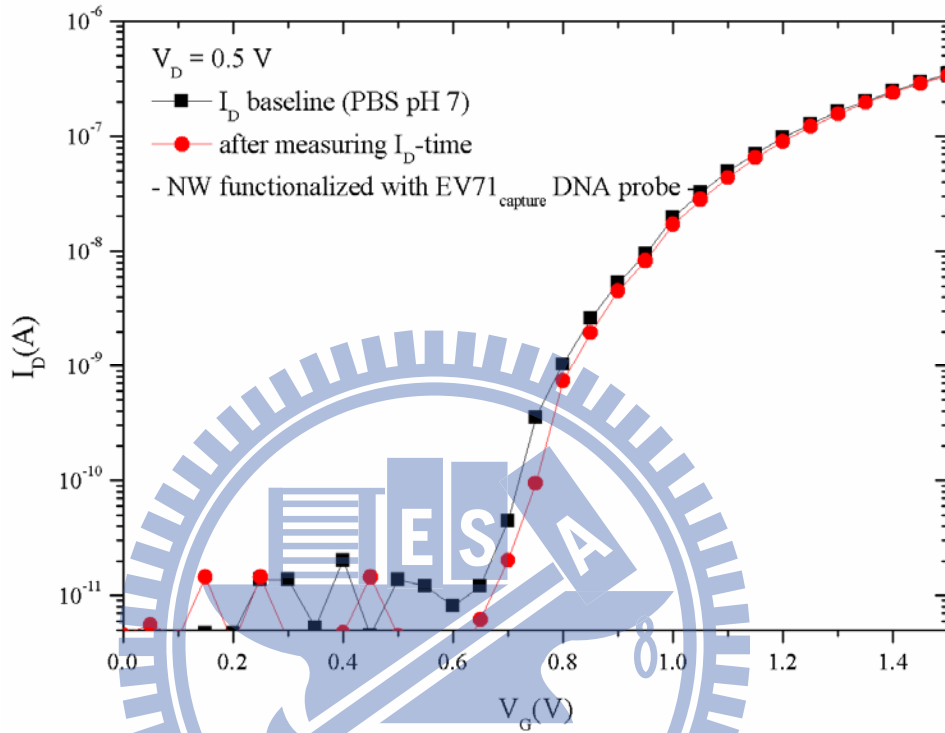


Figure 17 Electric responses of functionalized poly-SiNW FET to specific EV71_{target} in aqueous solution was determined before and after I_D -time measurement.

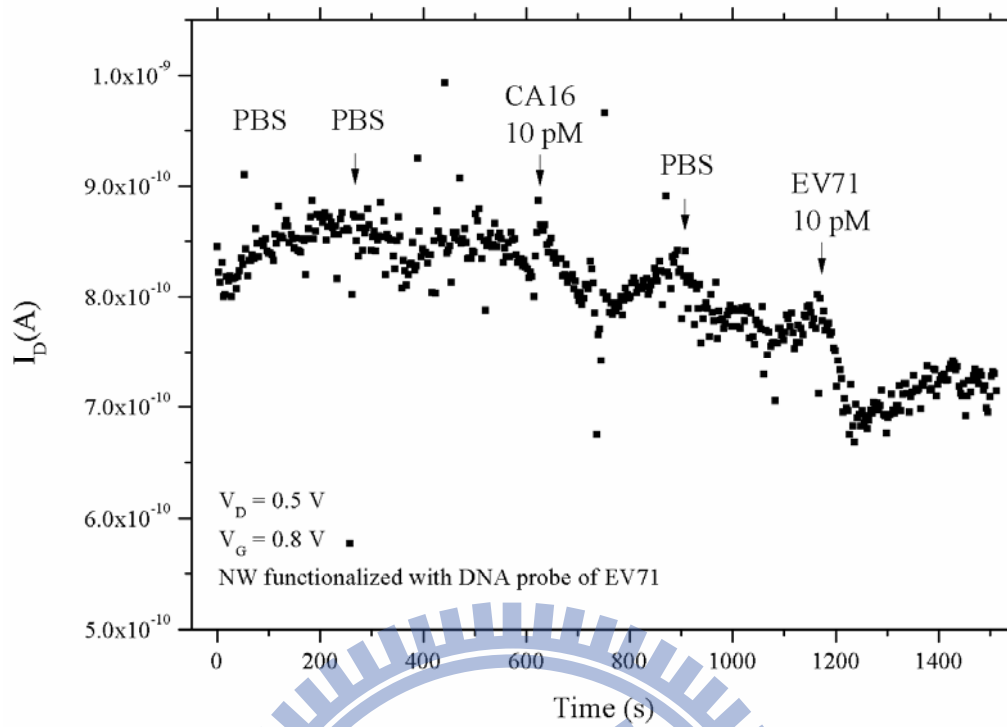
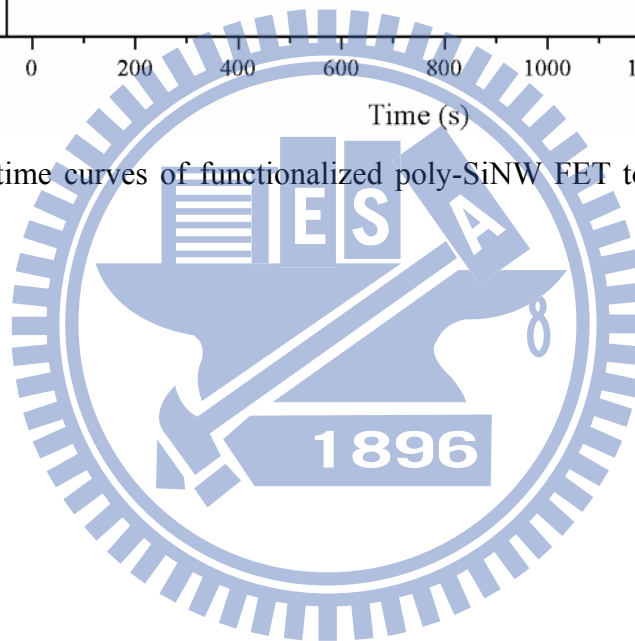


Figure 18 I_D -time curves of functionalized poly-SiNW FET to specific EV71_{target} in PBS.



3.2.3 NW immobilized with CA16_{capture} DNA probe and I_D-time curve was obtained with microfluidic system

The selectivity of functionalized poly SiNW-FET is shown in this section. Other captured DNAs, CA16_{capture}, were modified on the surface of poly SiNW-FET. The electric responses of the functionalized poly SiNW-FET were demonstrated to be dependent on the presence of CA16_{target}.

In Fig. 19 the I_D-V_G curves were obtained in PBS buffer (black square). To choose the I_D (about 10⁻⁹) was induced by V_G (0.75 V) in the linear region with great variation and starts to measure the electric response in the PBS buffer as I_D baseline. PBS buffer solution contained CA16_{target} (10 pM) and EV71_{target} (10 pM). PBS buffer, EV71_{target}, PBS, and CA16_{target} were injected into the channel (arrow indicated), respectively, and I_D-time curve was determined (Fig. 20). Adding PBS buffer as controlled experiments and continuously measured until it become stable without current shift to ensure that no further variation can be observed. When the electric response of PBS to surface of device was stable, then adding next flowing reagent and continuously measured about 300 seconds each reaction. When comparing current curve behavior to those controlled experiments, such as non-complementary EV71_{target} DNA and PBS buffer, we noted that the biosensing test gave the current shift is smaller than complementary CA16_{target} DNA hybridized with CA16_{capture} DNA probe, the current decrease was observed. After measuring I_D-time curve, the electric characteristic of the same device was shown in Fig. 19 (red circle). The range of current shift of before and after I_D-time measurement is matched between I_D-V_G curves and I_D-time curve.

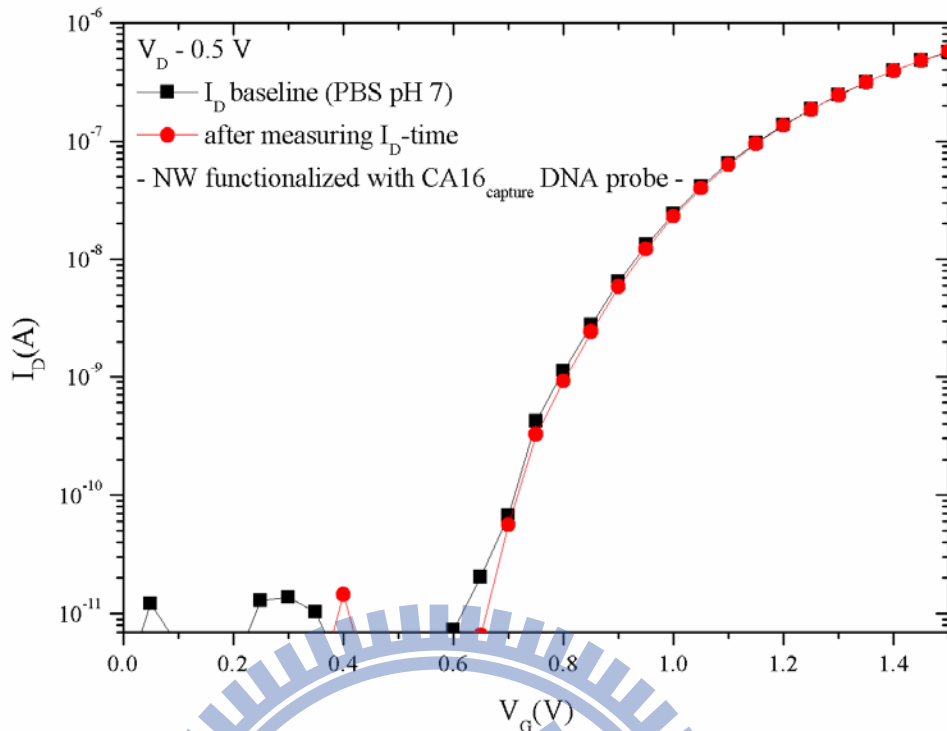


Figure 19 Electric responses of functionalized poly-SiNW FET to specific CA16_{target} in aqueous solution was determined before and after I_D -time measurement.

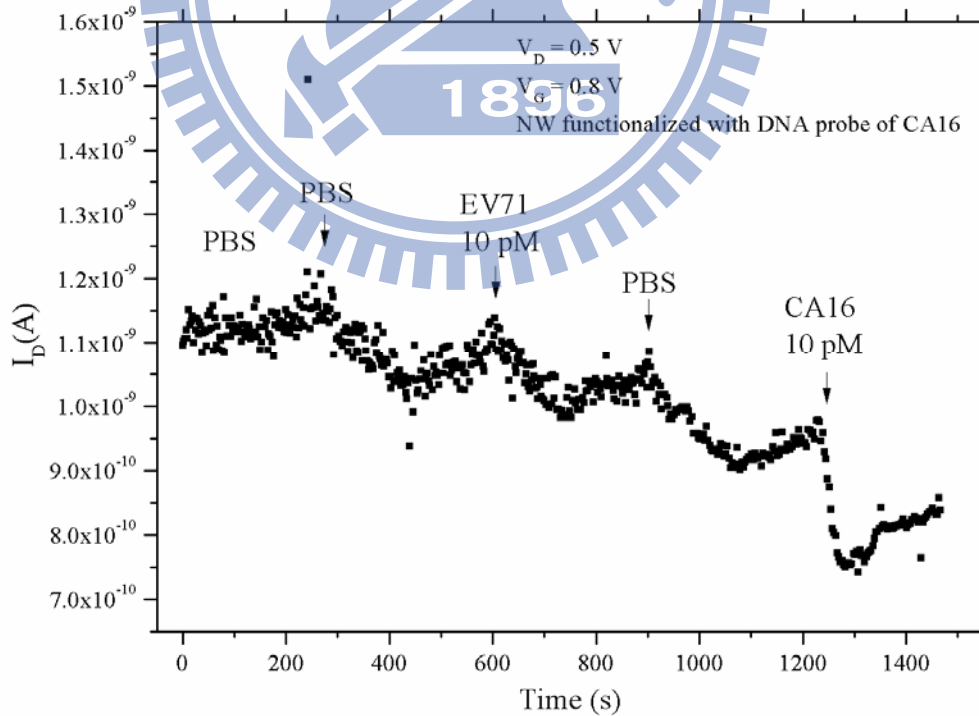


Figure 20 I_D -time curves of functionalized poly-SiNW FET to specific CA16_{target} in PBS.

The experimental method is the same as above and observed the same result which is shown in Fig. 21 and Fig. 22. These two experiments are still done in the same day. It also proves that the experiment is reproducible.

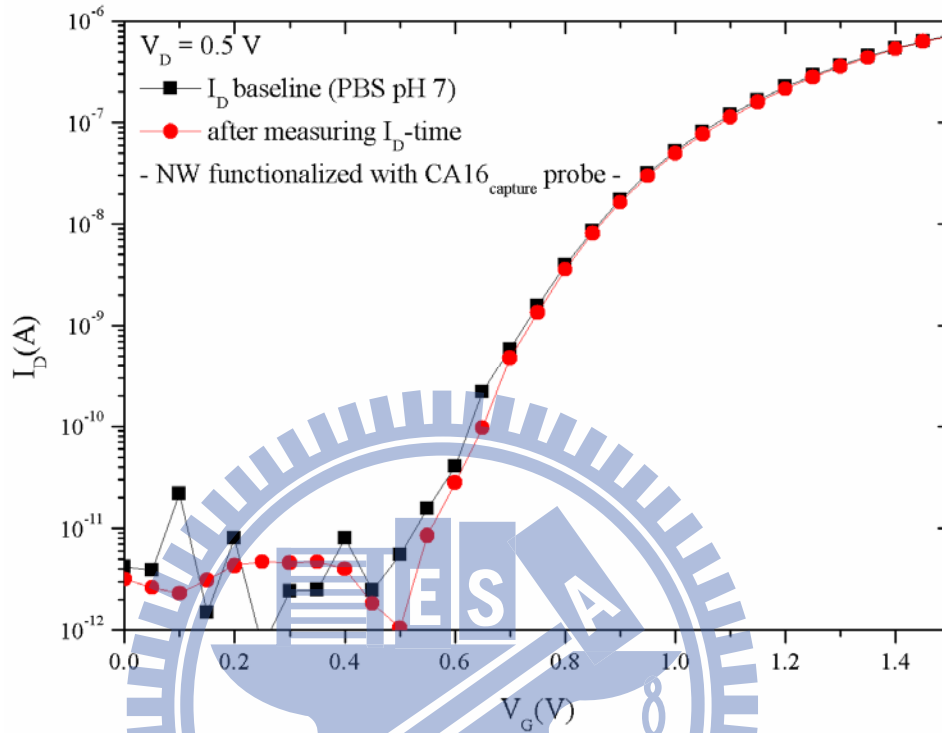


Figure 21 Electric responses of functionalized poly-SiNW FET to specific CA16_{target} in aqueous solution was determined before and after I_D -time measurement.

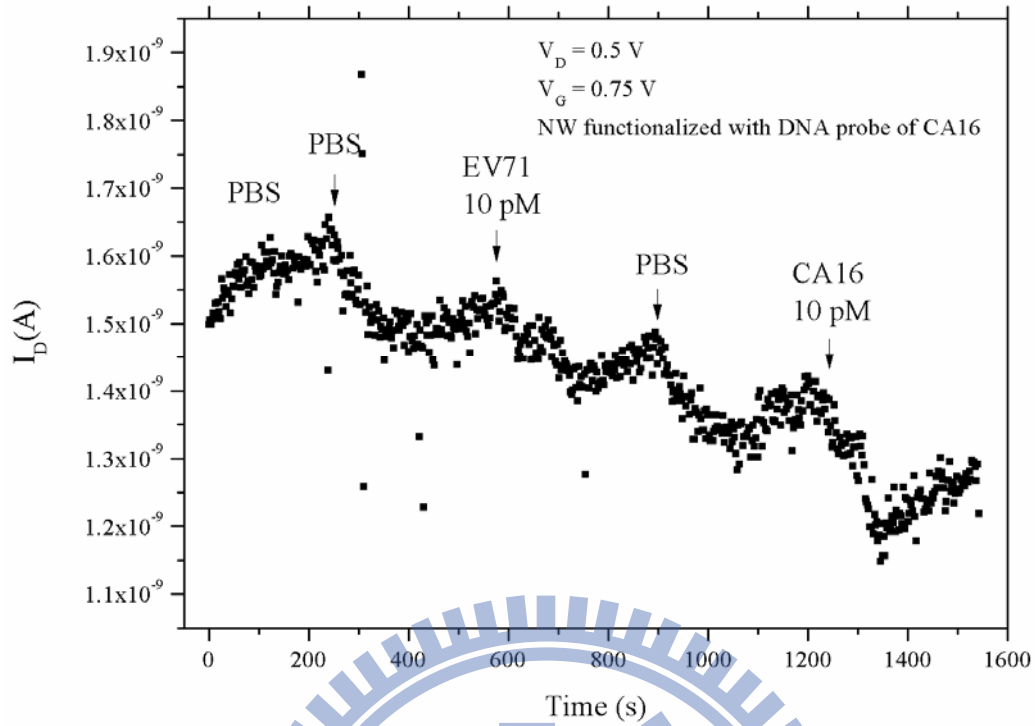
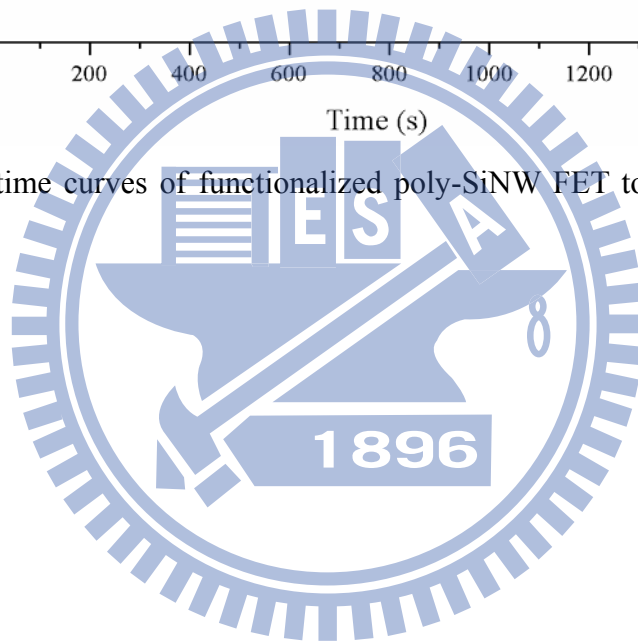


Figure 22 I_D-time curves of functionalized poly-SiNW FET to specific CA16_{target} in PBS.



3.2.4 Concentration-dependent electric response of EV71_{capture} functionalized poly-SiNW FET device

Sensitivity and specificity of functionalized poly SiNW-FET for biosensing DNA/DNA interactions are shown in Fig. 23 and 24. The increase in negative charges resulted from hybridization between EV71_{capture} and EV71_{target} can affect greatly the surface conductivity of SiNW-FET. For an N-type NW-FET, a decrease of the current will be expected when negative charges comes from phosphoric acid of DNA were introduced on sensing surface of n-type device[56]. In Fig. 23 the I_D - V_G curves were obtained in PBS buffer (black square), and following the addition of PBS, CA16 (10 pM), PBS and variety concentration of EV71, respectively. PBS and CA16 were load directly on the nanowire device with a microfluidic system as controlled experiments and continuously measured until it become stable without current shift to ensure that no further variation can be observed. However, when a complementary EV71_{target} hybridized with EV71_{capture} DNA probe, the current decrease was observed.

Controlled experiments with unmodified poly SiNW-FET are shown in Fig. 24. The current change-less in PBS, CA16_{target}, and EV71_{target} indicated that the electric characteristic was stable in the presence of non-interacting charged molecules.

The lowest detectable concentration and detection range of EV71_{target} with EV71_{capture} modified poly SiNW-FET was further demonstrated electric responses in Fig. 23. A constant V_D was set at 0.5 V for all the electric measurement. The I_D -time curves were determined as described above by using different concentrations of EV71_{target}. For the EV71_{capture} functionalized poly SiNW-FET, I_D -time curves were indistinguishable in PBS and in the presence of CA16_{target}. Concentration-dependent electric responses were observed for EV71_{target} concentration increasing from 100 aM to 100 fM. The concentration more increase, the influence on the current smaller was

evidences when $EV71_{target}$ concentration is 10 fM. This characteristic further confirmed that change of current in I_D -time curve was specifically affected by the interactions between $EV71_{target}$ and $EV71_{capture}$ on the SiNW surface. The I_D -time curve become change-less after saturation even much higher concentration of $EV71_{target}$ (100 fM) was added.

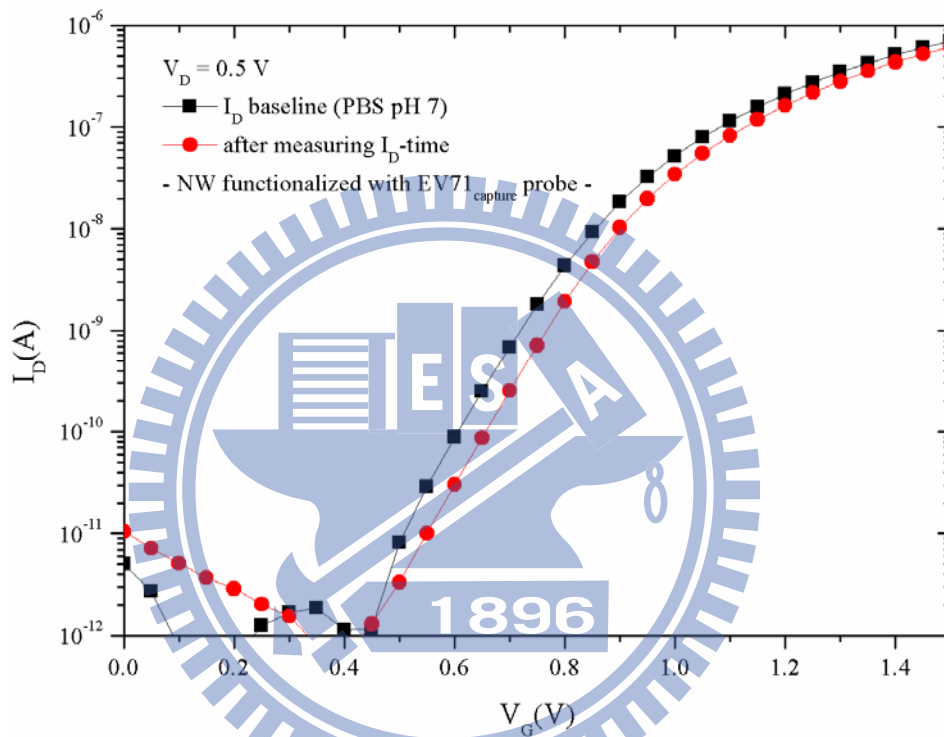


Figure 23 Electric responses of functionalized poly-SiNW FET to specific $EV71_{target}$ was determined before and after I_D -time measurement.

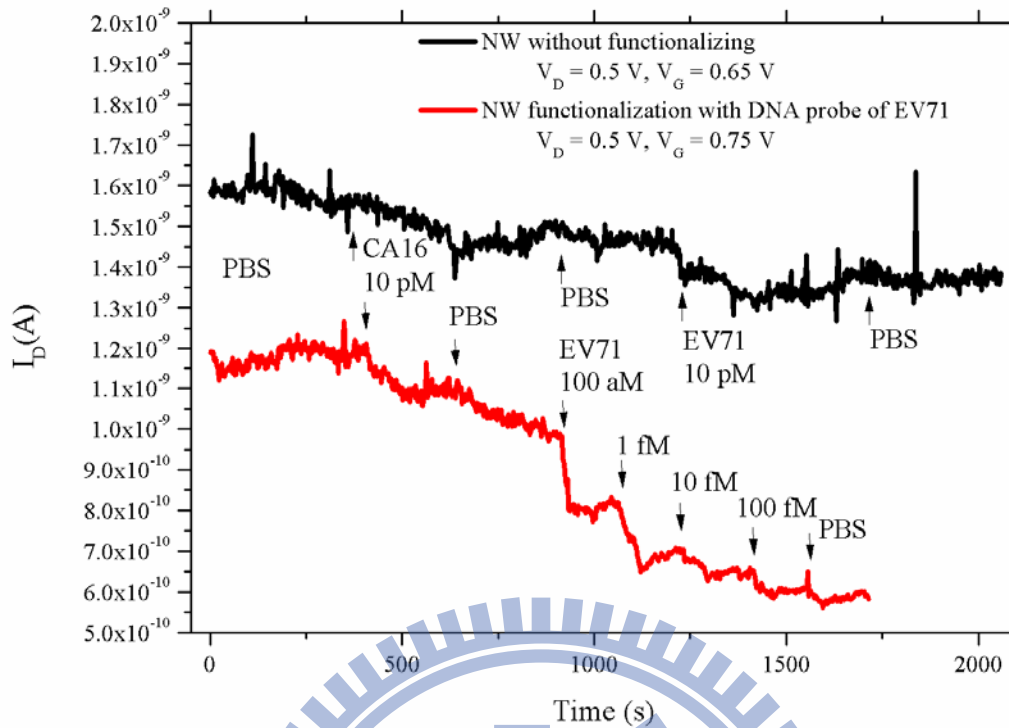
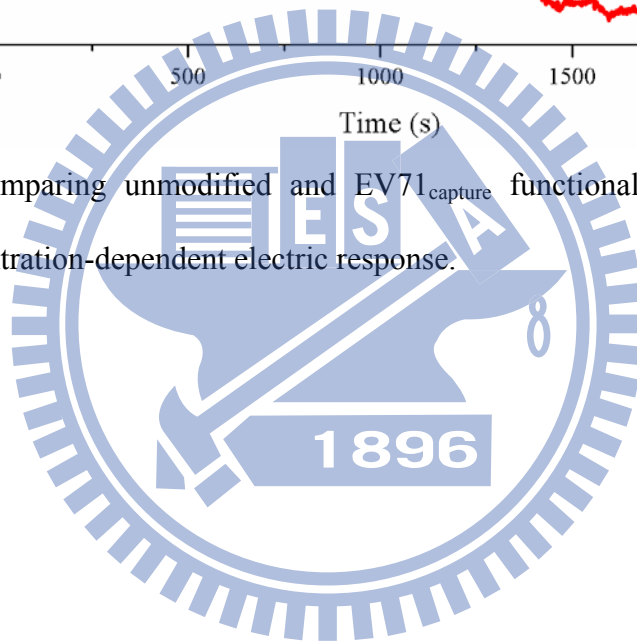


Figure 24 comparing unmodified and EV71_{capture} functionalized poly-SiNW FET device concentration-dependent electric response.



IV. Summary and perspective

In our research, we have demonstrated for the first time that a semiconductive poly SiNW-FET could be developed as a highly specific sensor for EV71 and CA16 nucleic acid with sensitivity in aM range. Throughout the fabrication of the poly SiNW-FET, no expensive lithography tools were need for definition of nanoscale patterns. Our result indicate the fabrication of poly SiNW-FET for sensitive and specific biosensing device can be achieved using commercially available procedures. Therefore, the poly SiNW-FET should has a great potential for real-time molecular diagnostics and direct surveillance of infection diseases



V. References

- [1] 行政院衛生署疾病管制局. "腸病毒感染併發重症(含非小兒麻痺病毒之腸病毒感染症)," http://www.cdc.gov.tw/index_info_info.asp?data_id=1007.
- [2] K. Y. Huang, and T. Y. Lin, "Enterovirus 71 infection and prevention," *Taiwan Epidemiology Bulletin*, 24, https://teb.cdc.gov.tw/main_e/news_list.aspx?id=2136, 2008].
- [3] T. Y. Lin, L. Y. Chang, S. H. Hsia *et al.*, "The 1998 enterovirus 71 outbreak in Taiwan: Pathogenesis and management," *Clinical Infectious Diseases*, vol. 34, pp. S52-S57, 2002.
- [4] King AM, Brown F, and Christian P, "Picornaviridae 2000, In Virus Taxonomy,," *Seventh Report of the International Committee on Taxonomy of Viruses*, pp. 657-678, San Diego: Academic Press.
- [5] T. Y. Lin, S. J. Twu, M. S. Ho *et al.*, "Enterovirus 71 outbreaks, Taiwan: occurrence and recognition," *Emerging Infectious Diseases*, vol. 9, no. 3, pp. 291-293, 2003.
- [6] S. F. Wang, "An epidemiological analysis of enterovirus 71: Taiwan, 1998-2004," *Taiwan Epidemiology Bulletin*, 21, https://teb.cdc.gov.tw/main/news_list.aspx?id=512, 2005].
- [7] H. S. Wu, Y. P. Huang, T. L. Lin *et al.*, "Update on the Molecular Epidemiology of Human Enterovirus 71 in Taiwan Since 1998," *International Journal of Infectious Diseases*, vol. 12, no. Supplement 1, 2008.
- [8] L. Chang, T. Lin, Y. Huang *et al.*, "Comparison of enterovirus 71 and coxsackie-virus A16 clinical illnesses during the Taiwan enterovirus epidemic, 1998," *The pediatric infectious disease journal*, vol. 18, no. 12, pp. 1092-1096, 1999.

- [9] 行政院衛生署疾病管制局, "腸病毒感染併發重症臨床處理注意事項," 2006].
- [10] "傳染病防治工作手冊-腸病毒感染併發重症," 台灣疾病管制局, 2008.
- [11] 行政院衛生署疾病管制局, "腸病毒感染防治手冊," 行政院衛生署疾病管制局, 2007.
- [12] Y. Wu, J. Xiang, C. Yang *et al.*, "Single-crystal metallic nanowires and metal/semiconductor nanowire heterostructures," *Nature*, vol. 430, no. 6995, pp. 61-65, 2004.
- [13] Schmidt NJ, Lennette EH, and H. HH, "An apparently new enterovirus isolated from patients with disease of the central nervous system," *The journal of infectious disease*, vol. 129, no. 3, pp. 304-309, 1974.
- [14] Deibel R, Gross LL, and C. DN, "Isolation of a new enterovirus" *Proceedings of the Society for Experimental Biology and Medicine*, vol. 148, no. 1, pp. 203-207, 1975.
- [15] Blomberg J, Lycke E, Ahlfors K *et al.*, "New enterovirus type associated with epidemic of aseptic meningitis and-or hand, foot, and mouth disease," *Lancet*, vol. 13, no. 2, pp. 112, 1974.
- [16] Tagaya I, and T. K, "Epidemic of hand, foot and mouth disease in Japan, 1972-1973: difference in epidemiologic and virologic features from the previous one," *Japanese journal of medical science & biology*, vol. 28, no. 4, pp. 231-234, 1975.
- [17] G. L. Gilbert, K. E. Dickson, M. J. Waters *et al.*, "Outbreak of enterovirus 71 infection in Victoria, Australia, with a high incidence of neurologic involvement," *Pediatric Infectious Disease Journal*, vol. 7, no. 7, pp. 484-488, 1988.
- [18] L. M. Shindarov, M. P. Chumakov, M. K. Voroshilova *et al.*, "Epidemiological,

- clinical and pathomorphological characteristics of epidemic poliomyelitis-like disease caused by enterovirus 71,” *Journal of Hygiene Epidemiology Microbiology and Immunology*, vol. 23, no. 3, pp. 284-295, 1979.
- [19] G. Nagy, S. Takatsy, E. Kukan *et al.*, “Virological diagnosis of enterovirus type 71 infections: experiences gained during an epidemic of acute CNS diseases in Hungary in 1978,” *Archives of Virology*, vol. 71, no. 3, pp. 217-227, 1982.
- [20] WHO, “Outbreak of hand, foot and mouth disease in Sarawak. Cluster of deaths among infants and young children,” *Weekly epidemiological record*, vol. 72, pp. 211-212, 1997.
- [21] M. T. Ho, E. R. Chen, K. H. Hsu *et al.*, “An epidemic of enterovirus 71 infection in Taiwan,” *New England Journal of Medicine*, vol. 341, no. 13, pp. 929-935, 1999.
- [22] WHO. "Enterovirus - non polio," <http://www.who.int/mediacentre/factsheets/fs174/en/index.html>.
- [23] S. R. Shih, M. S. Ho, K. H. Lin *et al.*, “Genetic analysis of enterovirus 71 isolated from fatal and non-fatal cases of hand, foot and mouth disease during an epidemic in Taiwan, 1998,” *Virus Research*, vol. 68, no. 2, pp. 127-136, 2000.
- [24] A. S. Rigonan, L. Mann, and T. Chonmaitree, “Use of monoclonal antibodies to identify serotypes of enterovirus isolates,” *Journal of Clinical Microbiology*, vol. 36, no. 7, pp. 1877-1881, 1998.
- [25] S. Manzara, M. Muscillo, G. La Rosa *et al.*, “Molecular identification and typing of enteroviruses isolated from clinical specimens,” *Journal of Clinical Microbiology*, vol. 40, no. 12, pp. 4554-4560, 2002.
- [26] T. C. Chen, G. W. Chen, C. A. Hsiung *et al.*, “Combining multiplex reverse transcription-PCR and a diagnostic microarray to detect and differentiate enterovirus 71 and coxsackievirus A16,” *Journal of Clinical Microbiology*, vol. 44,

- no. 6, pp. 2212-2219, 2006.
- [27] J. J. Yan, I. J. Su, P. F. Chen *et al.*, “Complete genome analysis of enterovirus 71 isolated from an outbreak in Taiwan and rapid identification of enterovirus 71 and coxsackievirus A16 by RT-PCR,” *Journal of Medical Virology*, vol. 65, no. 2, pp. 331-339, 2001.
- [28] S. M. Lipson, K. David, F. Shaikh *et al.*, “Detection of precytopathic effect of enteroviruses in clinical specimens by centrifugation-enhanced antigen detection,” *Journal of Clinical Microbiology*, vol. 39, no. 8, pp. 2755-2759, 2001.
- [29] C. Guney, E. Ozkaya, M. Yapar *et al.*, “Laboratory diagnosis of enteroviral infections of the central nervous system by using a nested RT-polymerase chain reaction (PCR) assay,” *Diagnostic Microbiology and Infectious Disease*, vol. 47, no. 4, pp. 557-562, 2003.
- [30] S. Y. Wang, T. L. Lin, H. Y. Chen *et al.*, “Early and rapid detection of enterovirus 71 infection by IgM-capture ELISA,” *Journal of Virological Methods*, vol. 119, no. 1, pp. 37-43, 2004.
- [31] K. A. Lim, and M. Benyeshmelnick, “Typing of viruses by combinations of antiserum pools- application to typing of enteroviruses (Coxsackie and Echo),” *Journal of Immunology*, vol. 84, no. 3, pp. 309-317, 1960.
- [32] K. C. Tsao, P. Y. Chang, H. C. Ning *et al.*, “Use of molecular assay in diagnosis of hand, foot and mouth disease caused by enterovirus 71 or coxsackievirus A 16,” *Journal of Virological Methods*, vol. 102, no. 1-2, pp. PII S0166-0934(01)00376-7, 2002.
- [33] J. T. Hu, M. Ouyang, P. D. Yang *et al.*, “Controlled growth and electrical properties of heterojunctions of carbon nanotubes and silicon nanowires,” *Nature*, vol. 399, pp. 48-51, 1999.

- [34] Y. Cui, and C. M. Lieber, "Functional nanoscale electronic devices assembled using silicon nanowire building blocks," *Science*, vol. 291, no. 5505, pp. 851-853, 2001.
- [35] C. Yi, W. Qingqiao, P. Hongkun *et al.*, "Nanowire nanosensors for highly sensitive and selective detection of biological and chemical species," *Science/Science*, vol. 293, no. 5533, pp. 1289-92, 2001.
- [36] J. Hahn, and C. M. Lieber, "Direct ultrasensitive electrical detection of DNA and DNA sequence variations using nanowire nanosensors," *Nano Letters*, vol. 4, no. 1, pp. 51-54, 2004.
- [37] F. Patolsky, G. F. Zheng, O. Hayden *et al.*, "Electrical detection of single viruses," *Proceedings of the National Academy of Sciences of the United States of America*, vol. 101, no. 39, pp. 14017-14022, 2004.
- [38] G. F. Zheng, F. Patolsky, Y. Cui *et al.*, "Multiplexed electrical detection of cancer markers with nanowire sensor arrays," *Nature Biotechnology*, vol. 23, no. 10, pp. 1294-1301, 2005.
- [39] F. Patolsky, B. P. Timko, G. H. Yu *et al.*, "Detection, stimulation, and inhibition of neuronal signals with high-density nanowire transistor arrays," *Science*, vol. 313, no. 5790, pp. 1100-1104, 2006.
- [40] Y. Chen, X. H. Wang, S. Erramilli *et al.*, "Silicon-based nanoelectronic field-effect pH sensor with local gate control," *Applied Physics Letters*, vol. 89, no. 22, pp. 223512, 2006.
- [41] S. Q. Lud, M. G. Nikolaidis, I. Haase *et al.*, "Field effect of screened charges: Electrical detection of peptides and proteins by a thin-film resistor," *Chemphyschem*, vol. 7, no. 2, pp. 379-384, 2006.
- [42] E. Stern, J. F. Klemic, D. A. Routenberg *et al.*, "Label-free immunodetection with

- CMOS-compatible semiconducting nanowires,” *Nature*, vol. 445, no. 7127, pp. 519-522, 2007.
- [43] S. S. Wong, E. Joselevich, A. T. Woolley *et al.*, “Covalently functionalized nanotubes as nanometre-sized probes in chemistry and biology,” *Nature*, vol. 394, no. 6688, pp. 52-55, 1998.
- [44] C. Campagnolo, K. J. Meyers, T. Ryan *et al.*, “Real-Time, label-free monitoring of tumor antigen and serum antibody interactions,” *Journal of Biochemical and Biophysical Methods*, vol. 61, no. 3, pp. 283-298, 2004.
- [45] G. H. Wu, R. H. Datar, K. M. Hansen *et al.*, “Bioassay of prostate-specific antigen (PSA) using microcantilevers,” *Nature Biotechnology*, vol. 19, no. 9, pp. 856-860, 2001.
- [46] H. Ogi, K. Motohisa, K. Hatanaka *et al.*, “High-frequency wireless and electrodeless quartz crystal microbalance developed as immunosensor,” *Japanese Journal of Applied Physics Part 1-Regular Papers Brief Communications & Review Papers*, vol. 46, no. 7B, pp. 4693-4697, 2007.
- [47] X. Michalet, F. F. Pinaud, L. A. Bentolila *et al.*, “Quantum dots for live cells, in vivo imaging, and diagnostics,” *Science*, vol. 307, no. 5709, pp. 538-544, 2005.
- [48] Y. C. Zhang, and A. Heller, “Reduction of the nonspecific binding of a target antibody and of its enzyme-labeled detection probe enabling electrochemical immunoassay of an antibody through the 7 pg/mL-100 ng/mL (40fM-400pM) range,” *Analytical Chemistry*, vol. 77, no. 23, pp. 7758-7762, 2005.
- [49] S. R. Shih, Y. W. Wang, G. W. Chen *et al.*, “Serotype-specific detection of enterovirus 71 in clinical specimens by DNA microchip array,” *Journal of Virological Methods*, vol. 111, no. 1, pp. 55-60, 2003.
- [50] C. Y. Hsiao, C. H. Lin, C. H. Hung *et al.*, “Novel poly-silicon nanowire field effect

- transistor for biosensing application,” *Biosensors & Bioelectronics*, pp. 1223-9, 2009.
- [51] H. C. Lin, M. H. Lee, C. J. Su *et al.*, “A simple and low-cost method to fabricate TFTs with poly-Si nanowire channel,” *Ieee Electron Device Letters*, vol. 26, no. 9, pp. 643-645, 2005.
- [52] C. J. Su, H. C. Lin, and T. Y. Huang, “High-performance TFTs with Si nanowire channels enhanced by metal-induced lateral crystallization,” *Ieee Electron Device Letters*, vol. 27, no. 7, pp. 582-584, 2006.
- [53] C. H. Lin, C. Y. Hsiao, C. H. Hung *et al.*, “Ultrasensitive detection of dopamine using a polysilicon nanowire field-effect transistor,” *Chemical Communications*, no. 44, pp. 5749-5751, 2008.
- [54] H. C. Lin, C. J. Su, C. Y. Hsiao *et al.*, “Water passivation effect on polycrystalline silicon nanowires,” *Applied Physics Letters*, vol. 91, no. 20, pp. 202113, 2007.
- [55] C. J. Su, H. C. Lin, H. H. Tsai *et al.*, “Operations of poly-Si nanowire thin-film transistors with a multiple-gated configuration,” *Nanotechnology*, vol. 18, no. 21, 2007.
- [56] Z. Li, Y. Chen, X. Li *et al.*, “Sequence-specific label-free DNA sensors based on silicon nanowires,” *Nano Letters*, vol. 4, no. 2, pp. 245-247, Feb, 2004.
- [57] C. H. Lin, C. H. Hung, C. Y. Hsiao *et al.*, “Poly-silicon nanowire field-effect transistor for ultrasensitive and label-free detection of pathogenic avian influenza DNA,” *Biosensors & Bioelectronics*, vol. 24, no. 10, pp. 3019-3024, 2009.

Appendix. DNA Immobilize to the Nanowire Surface

DNA probe + complementary DNA-FAM

1E : APTES + glutaraldehyde + DNA probe + ethanolamine + complementary DNA-FAM
1C : APTES + glutaraldehyde + X + ethanolamine + complementary DNA-FAM
2C : APTES + X + DNA probe + ethanolamine + complementary DNA-FAM

